activity is tightly linked to its pro-apoptotic function (Pietenpol *et al*., 1994). Consistent with this notion, majority of loss-of-function mutations of p53 in a variety of primary human tumors is detected within its DNA-binding domain (Hollstein *et al*., 1991; Levine *et al*., 1994) and *p53*-deficient mice developed spontaneous tumors (Donehower *et al*., 1992).

In the present study, we found that NEDL1 binds to the COOH-terminal region of p53 and enhances its transcriptional activity as well as pro-apoptotic function in its catalytic activity-independent manner. Our present findings suggest that NEDL1 plays a pivotal role in the induction of apoptosis in cancerous cells bearing wild-type *p53* through the interaction with p53 and also might provide a novel insight into understanding neuronal dysfunction.

Results

NEDL1 has a pro-apoptotic function

As described previously (Miyazaki *et al*., 2004), we cloned a novel gene termed *NEDL1* from the oligo-capping cDNA libraries prepared from a mixture of fresh primary neuroblastoma tissues that underwent spontaneous regression (Nakagawara and Ohira, 2004). *NEDL1* was highly expressed in favorable neuroblastomas as compared with unfavorable ones and significantly associated with better prognosis in neuroblastoma (Supplementary Figure S1). To examine the expression levels of NEDL1 in response to DNA damage, human neuroblastoma SH-SY5Y cells bearing wild-type *p53* were exposed to 20 μM of cisplatin (CDDP). At the indicated time periods, cells were subjected to terminal deoxynucleotidyl transferase-mediated dUTP-biotin nick end labeling (TUNEL) staining. As shown in Figure 1a, SH-SY5Y cells underwent apoptosis in a time-dependent manner. We then analysed the expression patterns of NEDL1 and p53 in response to CDDP. As shown in Figures 1b and c, p53 was induced to accumulate at protein level but not at mRNA level and CDDP treatment promoted phosphorylation of p53 at Ser-15 in association with a significant upregulation of various p53 target genes such as $p21^{WAF1}$, *Bax* and *Noxa*. It is noteworthy that NEDL1 increased at both mRNA and protein levels in SH-SY5Y cells exposed to CDDP in a time-dependent manner. *NEDL1* was also upregulated in *p53*-deficient human lung carcinoma H1299 cells in response to CDDP (Figure 1d), indicating that *NEDL1* might not be a direct target of p53. Since a correlation between expression levels of NEDL1 and p53 was observed in SH-SY5Y cells treated with CDDP, it is likely that there could exist a functional interaction between them during DNA damage-mediated apoptotic response.

To confirm this notion, we performed colony formation assay. *p53*-proficient SH-SY5Y, human osteosarcoma U2OS, *p53*-deficient human lung carcinoma H1299 and human osteosarcoma SAOS-2 cells were transfected

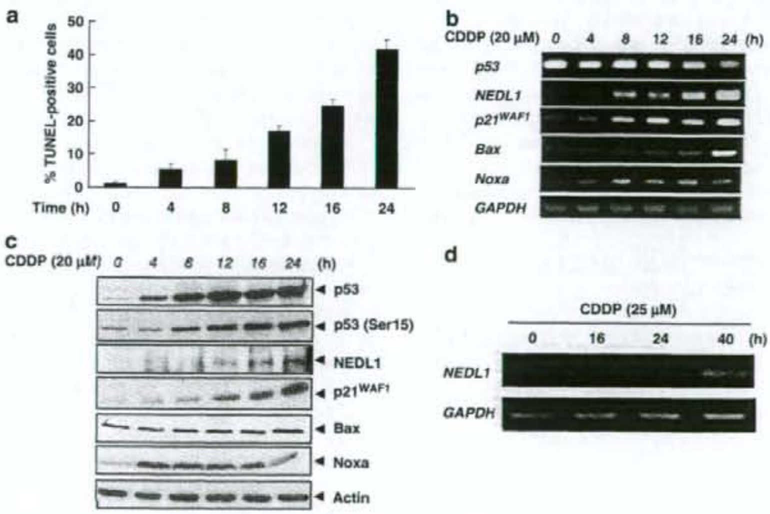

Figure 1 NEDL1 is induced to accumulate in response to CDDP. (**a**) CDDP-mediated apoptosis. SH-SY5Y cells were treated with CDDP (20 μM). Cells were then stained with an *in situ* cell death detection kit followed by mounting with 4′,6-diamidino-2-phenylindole-containing mounting medium. The number of TUNEL-positive cells was scored. Results were expressed as means ± s.d. of three independent experiments. (**b** and **c**) Expressions of NEDL1 and p53 in response to CDDP. Total RNA and cell lysates were prepared from SH-SY5Y cells exposed to CDDP for the indicated time periods and subjected to RT–PCR (**b**) and immunoblotting (**c**), respectively. (**d**) *NEDL1* is induced in *p53*-deficient H1299 cells exposed to CDDP. H1299 cells were treated with 25 μM of CDDP. At the indicated time points, total RNA was prepared and analysed for the expression levels of *NEDL1* by RT–PCR. *GAPDH* was used as an internal control. CDDP, cisplatin; GAPDH, glyceraldehyde-3-phosphate dehydrogenase; NEDL1, NEDD4-like ubiquitin protein ligase-1; RT–PCR, reverse transcription–PCR; TUNEL, terminal deoxynucleotidyl transferase-mediated dUTP-biotin nick end labeling.

with empty plasmid or with expression plasmid for NEDL1. Following 2 weeks of selection with G418, drug-resistant colonies were stained and photographed. As shown in Figures 2a and b, enforced expression of NEDL1 caused a significant decrease in the number of drug-resistant colonies in *p53*-proficient SH-SY5Y and U2OS cells relative to control cells, whereas NEDL1 had undetectable effects on *p53*-deficient H1299 and SAOS-2 cells, indicating that NEDL1 induces cell cycle arrest and/or apoptosis in cells carrying wild-type *p53*.

To address whether NEDL1 could cooperate with p53 to induce cell cycle arrest and/or apoptosis, we checked NEDL1-mediated proteolytic cleavage of caspase-3. For this purpose, expression plasmid for NEDL1 was introduced into the indicated cells. As shown in Figure 3a, NEDL1-mediated proteolytic cleavage of caspase-3 was detectable in SH-SY5Y and U2OS cells, but not in H1299 and SAOS-2 cells. Furthermore, enforced expression of NEDL1 resulted in an increase in the number of U2OS cells with sub-G1 DNA content (Figure 3b), whereas NEDL1 had negligible effects on SAOS-2 cells (Figure 3c). Since U2OS cells expressed wild-type p53, these findings suggest that NEDL1 induces apoptosis in a p53-dependent manner.

Interaction between NEDL1 and p53

To determine whether NEDL1 could interact with p53, COS7 cells were transfected with NEDL1 expression plasmid. As shown in Figure 4a, the anti-NEDL1 immunoprecipitates contained endogenous p53. To further confirm this issue, cell lysates prepared from U2OS cells exposed to CDDP were immunoprecipitated with normal rabbit serum or with anti-NEDL1 antibody and analysed by immunoblotting with anti-p53 antibody. As shown in Figure 4b, the anti-NEDL1 immunoprecipitates contained endogenous p53, suggesting that NEDL1 associates with endogenous p53 in cells. In contrast to wild-type p53, mutant form of p53 was not co-immunoprecipitated with NEDL1 (Figure 4c). To identify the region(s) of p53 responsible for the interaction with NEDL1, we performed *in vitro* pull-down assay using the indicated radio-labeled p53 deletion mutants. As clearly shown in Figure 4d, full-length p53, p53(1–353) and p53(102–393) were co-immunoprecipitated with NEDL1, whereas remaining p53 deletion mutants including p53(1–292) and p53(1–102) were not. Under our experimental conditions, other p53 family members such as p73 and p63 failed to be co-immunoprecipitated with NEDL1 (data not shown). These results suggest that NEDL1 specifically interacts with COOH-terminal region of p53 (amino-acid residues 293–353) and might modulate p53 function.

NEDL1 enhances the transcriptional activity of p53

Next, we sought to examine a possible effect of NEDL1 on the transcriptional activity of p53. H1299 cells were co-transfected with a constant amount of p53 expression plasmid, together with p53-responsive $p21^{WAF1}$ or *Bax* luciferase reporter construct in the presence or absence of increasing amounts of NEDL1 expression plasmid. As shown in Figures 5a and b, enforced expression of NEDL1 enhanced p53-mediated transactivation toward $p21^{WAF1}$ and *Bax* promoters in a dose-dependent manner. Similarly, luciferase activities driven by $p21^{WAF1}$ promoter were increased by NEDL1 in U2OS cells (Figure 5c). In support of these results, reverse transcription–polymerase chain reaction (RT–PCR) analysis showed that enforced expression of NEDL1 led to a significant increase in expression levels of endogenous $p21^{WAF1}$ and *Noxa* induced by exogenously

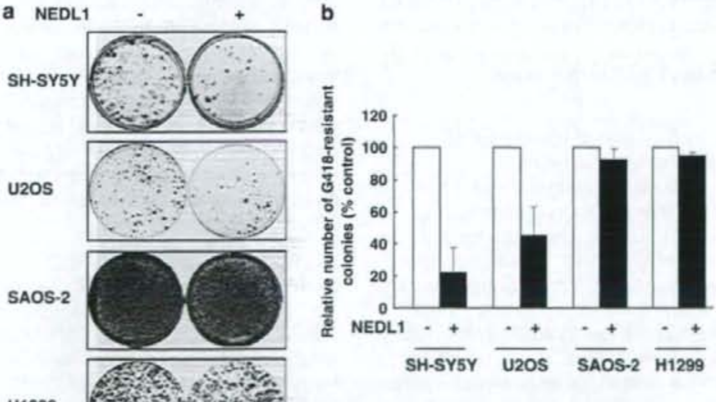

Figure 2 NEDL1 exerts its growth-suppressive and/or pro-apoptotic activity in cancerous cells bearing wild-type *p53*. (**a**) SH-SY5Y cells and U2OS cells harboring wild-type *p53* as well as *p53*-deficient H1299 cells and SAOS-2 cells were transfected with 2.0 μg of empty plasmid (pcDNA3) or with 2.0 μg of expression plasmid for NEDL1. Forty-eight hours after transfection, cells were transferred to fresh medium containing G418 (400 μg ml^{-1}). Two weeks after selection, drug-resistant colonies were stained with Giemsa's solution and photographed. (**b**) Average number of drug-resistant colonies in each transfection relative to pcDNA3 empty plasmid control (set at 100%). Results were expressed as means ± s.d. of three independent experiments. NEDL1, NEDD4-like ubiquitin protein ligase-1.

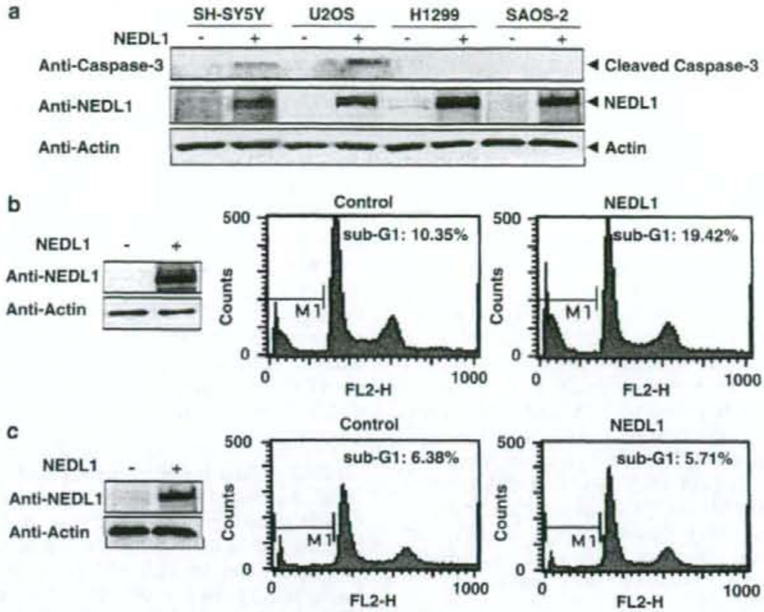

Figure 3 NEDL1 has a pro-apoptotic activity in cells bearing wild-type *p53*. (**a**) Cleavage of caspase-3. Expression plasmid encoding NEDL1 or empty plasmid was transfected into the indicated cells. Forty-eight hours after transfection, cell lysates were prepared and processed for immunoblotting with the indicated antibodies. (**b** and **c**) FACS analysis. U2OS (**b**) and SAOS-2 (**c**) cells were transfected with empty plasmid or with expression plasmid for NEDL1. Forty-eight hours after transfection, expression levels of NEDL1 were examined by immunoblotting (left panels) and number of cells with sub-G1 DNA content was analysed by FACS (right panels). NEDL1, NEDD4-like ubiquitin protein ligase-1.

expressed p53 (Figure 5d). Furthermore, chromatin immunoprecipitation (ChIP) assay demonstrated that NEDL1 has an ability to increase the amounts of exogenous and endogenous p53 recruited onto $p21^{WAF1}$ promoter region, whereas NEDL1 alone is not recruited onto $p21^{WAF1}$ promoter region (Figure 5e), indicating that NEDL1 might cooperate with p53 to directly induce the transcription of p53 target genes.

NEDL1 enhanced the pro-apoptotic activity of p53 independent of its ubiquitin ligase activity

Since NEDL1 has an intrinsic E3 ubiquitin ligase activity (Miyazaki *et al.*, 2004), these results prompted us to examine whether NEDL1 could ubiquitinate p53. In spite of our extensive efforts, we could not detect NEDL1-mediated ubiquitination of p53 (Supplementary Figure S2). Under our experimental conditions, NEDL1 efficiently ubiquitinated Dvl-1 as described previously (Miyazaki *et al.*, 2004), whereas HECT(−) mutant failed to ubiquitinate Dvl-1. To extend these observations, we examined a possible effect of NEDL1 catalytic activity on pro-apoptotic function of p53. H1299 cells were co-transfected with a constant amount of expression plasmid for p53 together with or without increasing amounts of wild-type NEDL1 or mutant form of NEDL1 lacking HECT domain termed HECT(−) (Figure 6a). Following 2 weeks of selection with G418 (400 μg ml^{-1}), drug-resistant colonies were stained with Giemsa's solution. Enforced expression of p53 decreased the number of drug-resistant colonies as compared with that in control cells (Figure 6b). As expected, coexpression of p53 plus wild-type NEDL1 or HECT(−) mutant led to a dramatic decrease in the number of drug-resistant colonies in a dose-dependent manner relative to that in cells expressing p53 alone. *In vitro* pull-down assay demonstrated that HECT(−) mutant, but not CW linker, retains an ability to interact with p53 (Figure 6c). In addition, CW linker had negligible effects on the transcriptional activity of p53 (Supplementary Figure S3). Thus, it is likely that NEDL1 enhances the transcriptional as well as pro-apoptotic function of p53 in its catalytic activity-independent manner.

siRNA-mediated knockdown of endogenous NEDL1 confers resistance of U2OS cells to adriamycin

To address the physiological role of endogenous NEDL1 in response to DNA damage, we designed small interfering RNAs (siRNAs) against NEDL1 termed nos. 1, 2, 3 and 4. U2OS cells were transfected with the indicated siRNAs. As shown in Figure 7a, nos. 2, 3 and 4 siRNAs successfully knocked down the endogenous *NEDL1*. We then used nos. 2 and 4 siRNAs for further experiments.

To examine the possible effect of siRNA targeting NEDL1 on the sensitivity to adriamycin (ADR), U2OS cells were transfected with control siRNA, no. 2 or 4 siRNA. Twenty-four hours after transfection, cells were

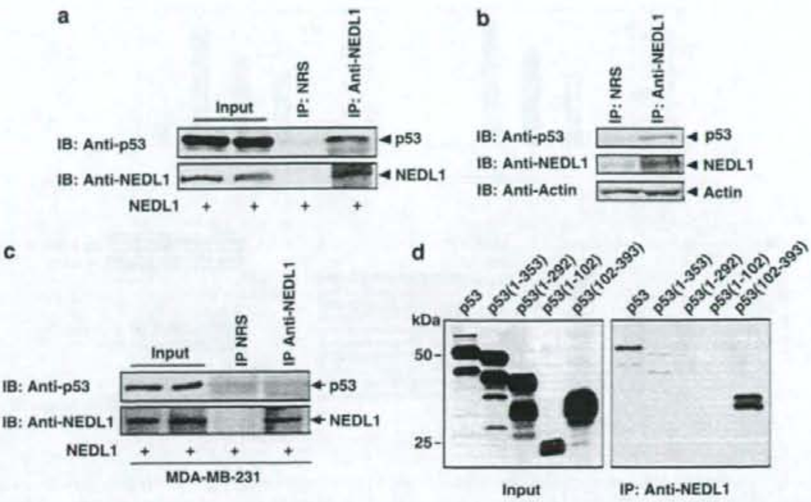

Figure 4 Interaction between NEDL1 and p53. (**a**) Immunoprecipitation. COS7 cells were transfected with NEDL1 expression plasmid. Forty-eight hours after transfection, cell lysates were prepared and immunoprecipitated with NRS or with polyclonal anti-NEDL1 antibody. Immunoprecipitates were analysed by immunoblotting with the indicated antibodies. Ten percentage of inputs were also loaded (input). (**b**) Endogenous interaction between NEDL1 and p53. U2OS cells were exposed to CDDP (20 μM). Twenty-four hours after CDDP treatment, cell lysates prepared from U2OS cells were immunoprecipitated with NRS or with anti-NEDL1 antibody and analysed by immunoblotting with anti-p53 antibody (top panel). The anti-NEDL1 immunoprecipitates contained endogenous NEDL1 (middle panel). To show that equal amounts of cell lysates are used for immunoprecipitation, expression of actin was examined (bottom panel). (**c**) Mutant form of p53 does not bind to NEDL1. Human breast cancer MDA-MB-231 cells, in which Arg at 280 is substituted with Lys, were transfected with expression plasmid for NEDL1. Forty-eight hours after transfection, cell lysates were immunoprecipitated with polyclonal anti-NEDL1 antibody or with NRS and the immunoprecipitates were analysed by immunoblotting with the indicated antibodies. Ten percentage of inputs are also shown (input). (**d**) The indicated p53 derivatives were labeled with [^{35}S]methionine *in vitro* and incubated with cell lysates prepared from COS7 cells transfected with expression plasmid for NEDL1. The reaction mixtures were immunoprecipitated with anti-NEDL1 antibody and the immunoprecipitates were analysed by sodium dodecyl sulfate–polyacrylamide gel electrophoresis. The gels were then dried and subjected to autoradiography. CDDP, cisplatin; NEDL1, NEDD4-like ubiquitin protein ligase-1; NRS, normal rabbit serum.

exposed to the indicated concentrations of ADR for 24 h followed by fluorescence-activated cell sorter (FACS) analysis. As shown in Figure 7b, U2OS cells transfected with control siRNA underwent apoptosis in a dose-dependent manner. In contrast, the number of cells with sub-G1 DNA content in response to ADR was significantly decreased in U2OS cells transfected with siRNAs against NEDL1 relative to cells expressing control siRNA. Similarly, siRNA-mediated knockdown of endogenous NEDL1 led to a remarkable decrease in the number of apoptotic cells caused by ADR in a time-dependent manner (Figure 7c).

Next, we determined whether siRNA-mediated knockdown of endogenous NEDL1 could inhibit the transcriptional activation of p53 target genes in response to ADR. U2OS cells were transfected with the indicated siRNAs. Twenty-four hours after transfection, cells were treated with ADR for 24 h. As shown in Figure 8a, ADR treatment induced the accumulation of p53 and phosphorylated form of p53 at Ser-15. However, siRNA-mediated knockdown of endogenous NEDL1 had negligible effects on amounts of p53 and phosphorylated form of p53 at Ser-15 in response to ADR, suggesting that their interaction does not affect the stability of p53 in response to DNA damage. It is noteworthy that expression levels of Noxa increased in cells exposed to ADR, whereas ADR-mediated upregulation of Noxa was markedly inhibited in NEDL1-knocked down U2OS cells. RT–PCR analysis also demonstrated that siRNA-mediated knockdown of endogenous NEDL1 reduces the transcription of p53 target genes such as *Noxa* and *Puma* induced by ADR (Figure 8b). ADR treatment had undetectable effects on *p53* (data not shown). Intriguingly, NEDL1 increased the acetylation levels of p73 (Figure 8c). Taken together, our present results suggest that NEDL1 has an ability to enhance the transcriptional and pro-apoptotic activities of p53 through the interaction without affecting its stability.

Discussion

In the present study, we have found that a novel HECT-type E3 ubiquitin ligase NEDL1 has the ability to cooperate with p53 to induce apoptosis.

During CDDP-mediated apoptosis in SH-SY5Y cells carrying wild-type *p53*, expression levels of NEDL1 correlated with those of p53. Expression levels of *NEDL1* were higher in favorable neuroblastoma than those in unfavorable neuroblastoma. Favorable neuroblastoma undergoes spontaneous regression through

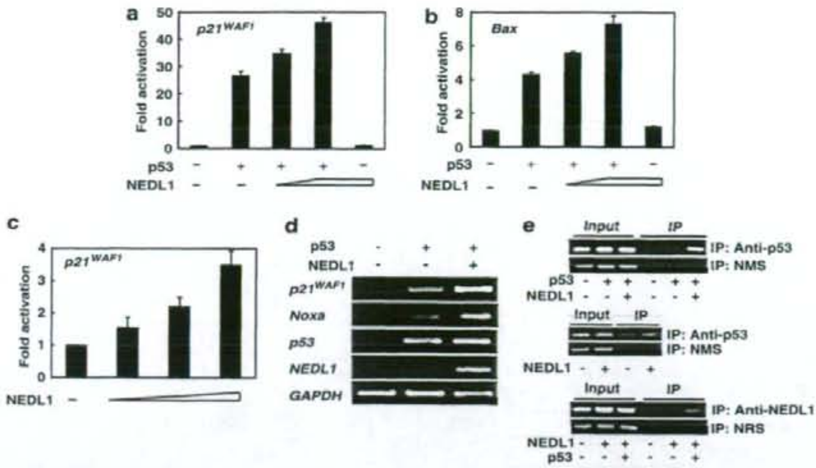

Figure 5 NEDL1 enhances the transcriptional activity of p53. (**a** and **b**) Luciferase reporter assays. H1299 cells were co-transfected with 25 ng of expression plasmid for p53, 100 ng of luciferase reporter construct containing p53-responsive element derived from *p21^{WAF1}* (**a**) or *Bax* (**b**) promoter and 10 ng of *Renilla* luciferase plasmid (pRL-TK) together with or without increasing amounts of expression plasmid for NEDL1 (475 and 875 ng). Total amount of plasmid DNA per transfection was kept constant (1 μg) with pcDNA3. Forty-eight hours after transfection, cell lysates were prepared and their luciferase activity was measured. Data were normalized to the *Renilla* luciferase activity. (**c**) Luciferase reporter assays. U2OS cells were co-transfected with 100 ng of luciferase reporter construct containing p53-responsive element derived from *p21^{WAF1}* promoter and 10 ng of pRL-TK together with or without increasing amounts of expression plasmid for NEDL1 (400, 800 and 1000 ng). Forty-eight hours after transfection, cell lysates were prepared and their luciferase activity was measured as described above. (**d**) RT–PCR analysis. H1299 cells were co-transfected with a constant amount of p53 expression plasmid (0.1 μg) along with or without NEDL1 expression plasmid (1.9 μg). Forty-eight hours after transfection, total RNA was isolated and subjected to RT–PCR analysis. *GAPDH* was used as an internal control. (**e**) ChIP assay. The increased binding of p53 to the promoter region of *p21^{WAF1}* caused by NEDL1 was demonstrated by ChIP assay with chromatin isolated from H1299 cells transfected with the indicated combinations of expression plasmids. As a control, PCR was performed on chromatin fragments isolated both before (input) and after (IP) immunoprecipitation with monoclonal anti-p53 antibody or with normal mouse serum (NMS) (upper panels). Middle panels show the increased binding of endogenous p53 to *p21^{WAF1}* promoter in the presence of NEDL1. Crosslinked chromatin isolated from U2OS cells transfected with or without NEDL1 expression plasmid exposed to adriamycin was subjected to ChIP assay. Lower panels show ChIP assay using crosslinked chromatin prepared from H1299 cells transfected with the indicated combinations of expression plasmids. Crosslinked chromatin was immunoprecipitated with polyclonal anti-NEDL1 or with NRS and subjected to PCR. CDDP, cisplatin; ChIP, chromatin immunoprecipitation; GAPDH, glyceraldehyde-3-phosphate dehydrogenase; NEDL1, NEDD4-like ubiquitin protein ligase-1; NRS, normal rabbit serum; RT–PCR, reverse transcriptase–PCR.

apoptosis and/or neuronal differentiation (Kitanaka *et al.*, 2002). In contrast to other human tumors, *p53* is rarely mutated in neuroblastoma (Moll *et al.*, 1995). Thus, it is likely that functional interaction between NEDL1 and p53 might contribute to induction of spontaneous regression caused by apoptosis of favorable neuroblastoma bearing wild-type *p53*. In support of this notion, enforced expression of NEDL1 reduced the number of drug-resistant colonies in cells with wild-type *p53* but not in *p53*-deficient cells. Furthermore, siRNA-mediated knockdown of endogenous NEDL1 inhibited DNA damage-induced apoptosis in cells bearing wild-type *p53*. Our present results demonstrated that NEDL1 binds to COOH-terminal region of p53 and enhances its transcriptional activation. In addition, NEDL1 increased the amounts of p53 recruited onto *p21^{WAF1}* promoter region. As described previously (Hupp and Lane, 1994), COOH-terminal region of p53 masked its DNA-binding domain to inhibit its transcriptional potential. Chemical modifications at COOH-terminal portion of p53, such as acetylation and glycosylation, lead to an increase in the transcriptional activity of p53 (Shaw *et al.*, 1996; Thomas and Chiang, 2005; Di Lello *et al.*, 2006). In accordance with this notion, enforced expression of NEDL1 resulted in an increase in acetylation levels of p53. Thus, it is possible that the interaction between NEDL1 and p53 might help to expose DNA-binding domain of p53 through the induction of acetylation of p53, and thereby enhance its transcriptional activity. However, the precise molecular mechanisms behind NEDL1-mediated induction of acetylation of p53 remained unclear. Further studies should be necessary to address this issue.

Although we found that NEDL1 has an intrinsic E3 ubiquitin ligase activity (Miyazaki *et al.*, 2004), our extensive efforts failed to detect NEDL1-mediated ubiquitination of p53 and enforced expression of NEDL1 had undetectable effects on the stability of endogenous p53 (data not shown). Under our experimental conditions, MDM2 promoted ubiquitination-mediated degradation of p53 (data not shown). NEDL1 and mutant form of NEDL1 lacking its catalytic HECT domain had an ability to decrease the number of drug-resistant colonies in H1299 cells co-transfected with p53 expression plasmid. Like wild-type NEDL1, this NEDL1 mutant retained an ability to interact with

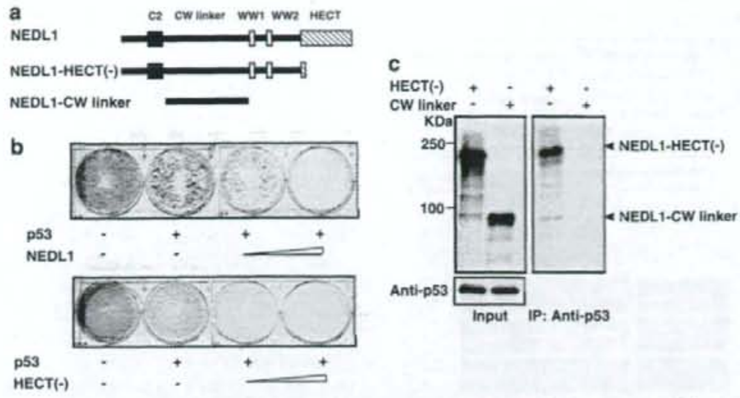

Figure 6 NEDL1 increases pro-apoptotic activity of p53 in its catalytic activity-independent manner. (**a**) Schematic diagram of wild-type NEDL1 and its deletion mutants. (**b**) Colony formation assay. H1299 cells were co-transfected with constant amount of p53 expression plasmid (25 ng) together with or without increasing amounts of expression plasmid for NEDL1 (475 and 975 ng) (upper panel) or NEDL1 lacking HECT domain (475 and 975 ng) (lower panel). Forty-eight hours after transfection, cells were grown in the fresh medium containing G418 (400 μg ml^{-1}). Following 2 weeks selection, drug-resistant colonies were stained with Giemsa's solution. (**c**) *In vitro* pull-down assay. Cell lysates prepared from COS7 cells were incubated with the indicated radio-labeled NEDL1 mutants and then immunoprecipitated with anti-p53 antibody. The immunoprecipitates were subjected to autoradiography (right panel). Left panel shows the autoradiography of the radio-labeled NEDL1 deletion mutants generated by *in vitro* transcription/translation system. NEDL1, NEDD4-like ubiquitin protein ligase-1.

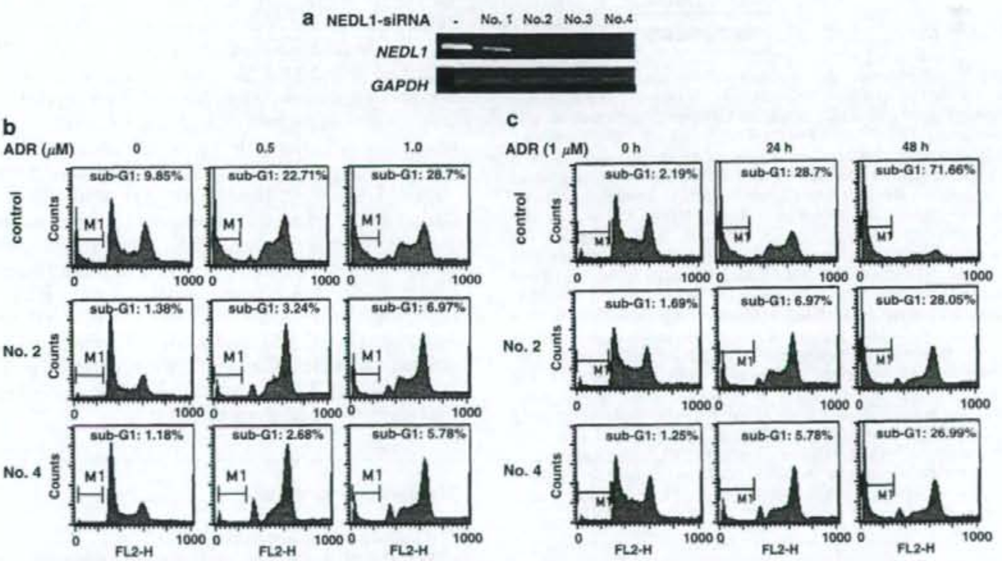

Figure 7 siRNA-mediated knockdown of endogenous NEDL1 confers resistance of U2OS cells to ADR. (**a**) siRNA-mediated knockdown of endogenous NEDL1. U2OS cells were transfected with control siRNA (−), siRNA against NEDL1 termed no. 1, 2, 3 or 4 siRNA. Forty-eight hours after transfection, total RNA was prepared and subjected to reverse transcriptase-PCR. *GAPDH* was used as an internal control. (**b**) U2OS cells were transfected with control siRNA, no. 2 or 4 siRNA. Twenty-four hours after transfection, cells were exposed to the indicated concentrations of ADR for 24 h and then cell cycle distributions of cells were analysed by FACS. (**c**) U2OS cells were transfected with control siRNA, no. 2 or 4 siRNA. Twenty-four hours after transfection, cells were treated with ADR (1 μM). At the indicated time periods, cell cycle distributions of cells were analysed by FACS. ADR, adriamycin; GAPDH, glyceraldehyde-3-phosphate dehydrogenase; NEDL1, NEDD4-like ubiquitin protein ligase-1; siRNA, small interfering RNA.

p53 but not ubiquitinate p53. Thus, it is conceivable that the interaction of NEDL1 with p53 suppresses the inhibitory effect of COOH-terminal region of p53 on its function in its catalytic activity-independent manner.

In contrast to p53, NEDL1 did not interact with other p53 family members such as p73 and p63 (data not shown). Intriguingly, we reported that NEDL2, a close relative to NEDL1, binds to PY motif of p73 and

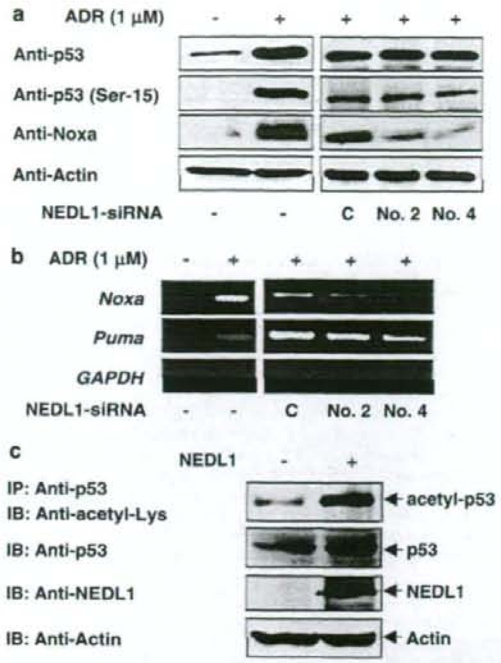

Figure 8 siRNA-mediated depletion of endogenous NEDL1 does not affect the stability of p53 but inhibits ADR-mediated upregulation of p53 target genes. (**a**) U2OS cells were treated with or without ADR (1 μM). Twenty-four hours after the treatment, cell lysates were prepared and subjected to immunoblotting with the indicated antibodies (left panels). U2OS cells were transfected with control siRNA (C), no. 2 or 4 siRNA. Twenty-four hours after transfection, cells were treated with ADR. At the indicated time periods, cell lysates were prepared and processed for immunoblotting with the indicated antibodies (right panels). (**b**) RT–PCR analysis. U2OS cells were treated as in (**a**), and total RNA was prepared and subjected to RT–PCR. (**c**) NEDL1-mediated increase in acetylation levels of p53. U2OS cells were transfected with empty plasmid or with expression plasmid for NEDL1. Forty-eight hours after transfection, cell lysates were immunoprecipitated with monoclonal anti-p53 antibody. The immunoprecipitates were analysed by immunoblotting with polyclonal anti-acetyl-Lys antibody (New England Biolabs, Ipswich, MA, USA). Expression levels of total p53, NEDL1 and actin were also examined. ADR, adriamycin; GAPDH, glyceraldehyde-3-phosphate dehydrogenase; NEDL1, NEDD4-like ubiquitin protein ligase-1; RT–PCR, reverse transcriptase–PCR; siRNA, small interfering RNA.

promotes ubiquitination of p73 (Miyazaki *et al*., 2003). According to our previous results, NEDL2-mediated ubiquitination of p73 increased the stability and activity of p73, raising a possibility that ubiquitination does not always act as a degradation signal. Consistent with our results, ubiquitination was required for the transcriptional activity of c-myc (Adhikary *et al*., 2005). It is noteworthy that NEDL2 did not interact with p53 that lacks PY motif and had negligible effects on p53 (Miyazaki *et al*., 2003), indicating that NEDL1 family members have a differential effect on p53 family members. In this regard, it is of interest to examine whether there could exist a functional interaction between NEDL1 family members and p63 that contains PY motif.

Several lines of evidence suggest that pro-apoptotic p53 signaling pathway is involved in motor neuron death associated with amyotrophic lateral sclerosis through an upregulation of pro-apoptotic Bax (Ekegren *et al*., 1999; Gonzalez de Aguilar *et al*., 2000; Martin and Liu, 2002). Recently, it has been shown that Noxa is one of the critical mediators of p53-dependent motor neuron death (Kiryo-Seo *et al*., 2005). These observations suggest that pro-apoptotic p53 signaling pathway plays a causable role in the regulation of neuronal cell death. Thus, it is likely that NEDL1 is involved in the regulation of this cellular process through the interaction with p53.

As described previously (Miyazaki *et al*., 2004), we found that Dvl-1, a highly conserved cytoplasmic phosphoprotein implicated in Wnt signaling pathway, is one of the physiological targets of NEDL1. On the basis of our previous results, NEDL1 ubiquitinated Dvl-1 and induced its degradation in a proteasome-dependent manner. It has been well documented that Dvl-1 increases the stability of β-catenin through the inhibition of the catalytic activity of glycogen synthase kinase-3β (GSK-3β) (Kishida *et al*., 2001; Lee *et al*., 2001; Hino *et al*., 2003). In addition, GSK-3β facilitated staurosporine-mediated apoptosis in SH-SY5Y cells (Bijur *et al*., 2000) and also contributed to neuronal apoptosis induced by trophic withdrawal (Hetman *et al*., 2000). Consistent with these results, specific inhibition of GSK-3β activity by a small chemical compound protected primary neuron from apoptosis (Cross *et al*., 2001). These results suggest that GSK-3β activity is closely involved in the induction of neuronal cell death. It is worth noting that GSK-3β interacts with p53 in response to DNA damage and enhances pro-apoptotic function of p53 (Watcharasit *et al*., 2002). Taken together, there exists a functional interaction among NEDL1, Dvl-1, p53 and GSK-3β, which might play a pivotal role at least in part in the regulation of apoptosis in response to DNA damage. Further studies should be necessary to address this issue.

Materials and methods

Cell culture and transfection

COS7, U2OS and SAOS-2 cells were maintained in Dulbecco's modified Eagle's medium supplemented with 10% of heat-inactivated fetal bovine serum (Invitrogen, Carlsbad, CA, USA), penicillin (100 IU ml^{-1}) and streptomycin (100 μg ml^{-1}). *p53*-deficient H1299 and SH-SY5Y cells were grown in RPMI-1640 medium supplemented with 10% heat-inactivated fetal bovine serum and antibiotic mixture. Cells were cultured at 37 °C in a water-saturated atmosphere of 95% air and 5% CO_2. Transient transfection was performed using LipofectAMINE 2000 transfection reagent (Invitrogen) according to the manufacturer's instructions.

Immunoblotting and immunoprecipitation

For immunoblotting, cells were lysed in a lysis buffer containing 25 mM Tris-Cl pH 7.5, 137 mM NaCl, 2.7 mM

KCl, 1% Triton X-100 and protease inhibitor cocktail. Equal amounts of cell lysates were separated by sodium dodecyl sulfate–polyacrylamide gel electrophoresis (SDS–PAGE) and transferred onto Immobilon-P membranes (Millipore, Bedford, MA, USA). The transferred membranes were incubated with monoclonal anti-p21^{WAF1} (Ab-1, Oncogene Research Products, Cambridge, MA, USA), monoclonal anti-p53 (DO-1, Oncogene Research Products), monoclonal anti-Noxa (ab13654, Abcom, Cambridge, UK), polyclonal anti-Bax (Cell Signaling, Beverly, MA, USA), polyclonal anti-caspase-3 (Calbiochem, San Diego, CA, USA), polyclonal anti-phosphorylated p53 at Ser-15 (Cell Signaling), polyclonal anti-NEDL1 or with polyclonal anti-actin (20–33, Sigma, St Louis, MO, USA) antibody followed by incubation with the appropriate HRP-conjugated secondary antibodies (Jackson ImmunoResearch Laboratories, West Grove, PA, USA). Bound antibodies were detected by ECL system (Amersham Biosciences, Piscataway, NJ, USA). For immunoprecipitation, 1 mg of protein was incubated with protein G-Sepharose beads (Amersham Biosciences). The precleaned lysates were incubated with polyclonal anti-NEDL1 antibody for 2 h at 4 °C and immunocomplexes were precipitated with protein G-Sepharose beads for additional 1 h at 4 °C. The immunocomplexes were washed three times with the lysis buffer, eluted from beads by adding 2 × SDS sample buffer, resolved by SDS–PAGE and subjected to immunoblotting with polyclonal anti-NEDL1 or with monoclonal anti-p53 (DO-1, Oncogene Research Products) antibody.

In vitro binding assay
Wild-type p53 and its deletion mutants were expressed *in vitro* using a T7 Quick Coupled Transcription/Translation System (Promega, Madison, WI, USA) in the presence of [^{35}S]methionine according to the manufacturer's recommendations. Cell lysates prepared from COS7 cells transfected with the expression plasmid encoding NEDL1 were mixed and incubated overnight at 4 °C. Reaction mixtures were then immunoprecipitated with the anti-NEDL1 antibody. Immunoprecipitates were washed extensively with the lysis buffer and resolved by SDS–PAGE. The gels were dried and subjected to autoradiography.

TUNEL assay
SH-SY5Y cells were grown on coverslips and treated with CDDP (20 μM). At the indicated time periods after the treatment with CDDP, cells were fixed in 4% paraformaldehyde and apoptotic cells were detected by using an *in situ* cell death detection Kit (Roche Molecular Biochemicals, Mannheim, Germany) according to the manufacturer's protocol. The coverslips were mounted with 4′,6-diamidino-2-phenylindole-containing mounting medium (Vector Laboratories, Burlingame, CA, USA) and observed under a Fluoview laser scanning confocal microscope (Olympus, Tokyo, Japan).

FACS analysis
U2OS and SAOS-2 cells were transfected with the expression plasmid for NEDL1. Forty-eight hours after transfection, floating and attached cells were collected, washed in phosphate-buffered saline and fixed in 70% ethanol at −20 °C. Following incubation in phosphate-buffered saline containing 40 μg ml^{-1} of propidium iodide and 200 μg ml^{-1} of RNase A for 1 h at room temperature in the dark, stained nuclei were analysed on a FACScan machine (Becton Dickingson, Mountain View, CA, USA).

RT–PCR
SH-SY5Y cells were treated with CDDP (20 μM). At the indicated time periods after the treatment, total RNA was prepared using an RNeasy mini kit (Qiagen, Valencia, CA, USA). Five micrograms of total RNA were employed to synthesize the first-strand cDNA by using random primers and SuperScript II reverse transcriptase (Invitrogen) according to the manufacturer's instructions. The resultant cDNA was subjected to the PCR-based amplification. The list of primer sets used will be provided upon request. The expression of glyceraldehyde-3-phosphate dehydrogenase was measured as an internal control. The PCR products were subjected to agarose gel electrophoresis and visualized by ethidium bromide staining.

Luciferase reporter assay
H1299 cells were allowed to adhere overnight in 12-well cell culture plates at a final density of 50 000 cells per well. Cells were then co-transfected with 25 ng of the p53 expression plasmid, 100 ng of the p53-responsible luciferase reporter construct (*p21^{WAF1}* or *Bax*) and 10 ng of pRL-TK *Renilla* luciferase cDNA together with or without increasing amounts of the NEDL1 expression plasmid (475 and 875 ng). Total amount of plasmid DNA per transfection was kept constant (1 μg) with an empty plasmid pcDNA3 (Invitrogen). Forty-eight hours after transfection, cells were lysed and both the firefly and *Renilla* luciferase activities were measured with dual-luciferase reporter assay system (Promega), according to the manufacturer's instructions. The firefly luminescence signal was normalized based on the *Renilla* luminescence signal.

Chromatin immunoprecipitation assay
Chromatin immunoprecipitation assay was performed according to the protocol provided by Upstate Biotechnology (Lake Placid, NY, USA). In brief, H1299 cells were transfected with the expression plasmid for p53 together with or without the expression plasmid for NEDL1. Forty-eight hours after transfection, cells were treated with 1% formaldehyde at 37 °C for 15 min. After being washed with ice-cold phosphate-buffered saline, cells were suspended with 200 μl of SDS lysis buffer (1% SDS, 10 mM EDTA and 50 mM Tris-HCl, pH 8.1) on ice for 10 min. Lysates were sonicated and insoluble materials were removed by centrifugation. Supernatants were then precleared with 20 μl of protein A agarose beads that had been preabsorbed with salmon sperm DNA at 37 °C for 30 min. The precleared chromatin solutions were immunoprecipitated with normal mouse serum or with anti-p53 antibody at 4 °C overnight, followed by incubation with 60 μl of protein A agarose beads for 1 h at 4 °C. Samples were eluted with 200 μl of the elution buffer (1% SDS and 0.1 M $NaHCO_3$) and then crosslinks were reversed by heating them at 65 °C for 6 h. Chromatin-associated proteins were digested with proteinase K at 45 °C for 1 h, and immunoprecipitated DNA was purified by using QIAquick PCR purification kit (Qiagen) according to the manufacturer's instructions. Purified DNA was analysed by PCR-based amplification. The primer set used to detect *p21^{WAF1}* promoter was as follows: 5′-CACCTTTCACCATTCCCCTA-3′ (forward) and 5′-GCAGCCCAAGGACAAAATAG-3′ (reverse).

Small interfering RNA
U2OS cells were transiently transfected with siRNA targeting NEDL1 (no. 1, 5′-CUAAAUGACUGGCGGAAUAUU-3′; no. 2, 5′-GAUGAGGUCUUGUCCGAAAUU-3′; no. 3, 5′-GAUGCCAGCUCGUACUUUGUU-3′; no. 4, 5′-CAGCUGCAAUUCCGAUUUGUU-3′) or control non-targeting

siRNA (Dharmacon, Chicago, IL, USA) by using Lipofect AMINE RNAiMAX transfection reagent (Invitrogen) according to the manufacturer's instructions. Forty-eight hours after transfection, total RNA was prepared and subjected to RT–PCR.

Colony formation assay
H1299, SH-SY5Y, U2OS and SAOS-2 cells were seeded at a final density of 1×10^5 cells per six-well dish and allowed to attach overnight. Cells were then co-transfected with the indicated combinations of the expression plasmids. Total amount of plasmid DNA per transfection was kept constant (2 μg) with pcDNA3. Forty-eight hours after transfection, cells were transferred to the fresh medium containing G418 (400 μg ml^{-1}). After 14 days, viable colonies were washed in phosphate-buffered saline and stained with Giemsa's solution.

Acknowledgements

We are grateful to Dr T Kamijo (Division of Biochemistry, Chiba Cancer Center Research Institute) for his helpful discussion. This work was supported in part by a grant-in-aid from the Ministry of Health, Labour and Welfare for Third Term Comprehensive Control Research for Cancer, a grant-in-aid for Scientific Research on Priority Areas from the Ministry of Education, Culture, Sports, Science and Technology, Japan, a grant-in-aid for Scientific Research from Japan Society for the Promotion of Science and Uehara Memorial Foundation.

References

Adhikary S, Marinoni F, Hock A, Hulleman E, Popov N, Beier R *et al.* (2005). The ubiquitin ligase HectH9 regulates transcriptional activation by Myc and is essential for tumor cell proliferation. *Cell* **123**: 409–421.

Bijur GN, De Sarno P, Jope RS. (2000). Glycogen synthase kinase-3beta facilitates staurosporine- and heat shock-induced apoptosis. *J Biol Chem* **275**: 7583–7590.

Cluskey S, Ramsden DB. (2001). Mechanisms of neurodegeneration in amyotrophic lateral sclerosis. *Mol Pathol* **54**: 386–392.

Cross DA, Culbert AA, Chalmers KA, Facci L, Skaper SD, Reith AD. (2001). Selective small-molecule inhibitors of glycogen synthase kinase-3 activity protect primary neurones from death. *J Neurochem* **77**: 94–102.

Di Lello P, Jenkins LM, Jones TN, Nguyen BD, Hara T, Yamaguchi H *et al.* (2006). Structure of the Tfb1/p53 complex: Insights into the interaction between the p62/Tfb1 subunit of TFIIH and the activation domain of p53. *Mol Cell* **22**: 731–740.

Donehower LA, Harvey M, Slagle BL, McArthur MJ, Montgomery Jr CA, Butel JS *et al.* (1992). Mice deficient for p53 are developmentally normal but susceptible to spontaneous tumours. *Nature* **356**: 215–221.

Ekegren T, Grundstrom E, Lindholm D, Aquilonius SM. (1999). Upregulation of Bax protein and increased DNA degradation in ALS spinal cord motor neurons. *Acta Neurol Scand* **100**: 317–321.

Gonzalez de Aguilar JL, Gordon JW, Rene F, de Tapia M, Lutz-Bucher B, Gaiddon C *et al.* (2000). Alteration of the Bcl-x/Bax ratio in a transgenic mouse model of amyotrophic lateral sclerosis: evidence for the implication of the p53 signaling pathway. *Neurobiol Dis* **7**: 406–415.

Hetman M, Cavanaugh JE, Kimelman D, Xia Z. (2000). Role of glycogen synthase kinase-3beta in neuronal apoptosis induced by trophic withdrawal. *J Neurosci* **20**: 2567–2574.

Hino S, Michiue T, Asashima M, Kikuchi A. (2003). Casein kinase I epsilon enhances the binding of Dvl-1 to Frat-1 and is essential for Wnt-3a-induced accumulation of beta-catenin. *J Biol Chem* **278**: 14066–14073.

Hollstein M, Sidransky D, Vogelstein B, Harris CC. (1991). p53 mutations in human cancers. *Science* **253**: 49–53.

Hupp TR, Lane DP. (1994). Regulation of the cryptic sequence-specific DNA-binding function of p53 by protein kinases. *Cold Spring Harb Symp Quant Biol* **59**: 195–206.

Kiryo-Seo S, Hirayama T, Kato R, Kiyama H. (2005). Noxa is a critical mediator of p53-dependent motor neuron death after nerve injury in adult mouse. *J Neurosci* **25**: 1442–1447.

Kishida M, Hino S, Michiue T, Yamamoto H, Kishida S, Fukui A *et al.* (2001). Synergistic activation of the Wnt signaling pathway by Dvl and casein kinase Iepsilon. *J Biol Chem* **276**: 33147–33155.

Kitanaka C, Kato K, Ijiri R, Sakurada K, Tomiyama A, Noguchi K *et al.* (2002). Increased Ras expression and caspase-independent neuroblastoma cell death: possible mechanism of spontaneous neuroblastoma regression. *J Natl Cancer Inst* **94**: 358–368.

Lee E, Salic A, Kirschner MW. (2001). Physiological regulation of [beta]- catenin stability by Tcf3 and CK1epsilon. *J Cell Biol* **154**: 983–993.

Levine AJ, Chang A, Dittmer D, Notterman DA, Silver A, Thorn K *et al.* (1994). The p53 tumor suppressor gene. *J Lab Clin Med* **123**: 817–823.

Martin LJ. (2000). p53 is abnormally elevated and active in the CNS of patients with amyotrophic lateral sclerosis. *Neurobiol Dis* **7**: 613–622.

Martin LJ, Liu Z. (2002). Injury-induced spinal motor neuron apoptosis is preceded by DNA single-strand breaks and is p53- and bax-dependent. *J Neurobiol* **5**: 181–197.

Miyazaki K, Fujita T, Ozaki T, Kato C, Kurose Y, Sakamoto M *et al.* (2004). NEDL1, a novel ubiquitin-protein isopeptide ligase for dishevelled-1, targets mutant superoxide dismutase-1. *J Biol Chem* **279**: 11327–11335.

Miyazaki K, Ozaki T, Kato C, Hanamoto T, Fujita T, Irino S *et al.* (2003). A novel HECT-type E3 ubiquitin ligase, NEDL2, stabilizes p73 and enhances its transcriptional activity. *Biochem Biophys Res Commun* **308**: 106–113.

Moll UM, LaQuaglia M, Benard J, Riou G. (1995). Wild-type p53 protein undergoes cytoplasmic sequestration in undifferentiated neuroblastomas but not in differentiated tumors. *Proc Natl Acad Sci USA* **92**: 4407–44011.

Nakagawara A, Ohira M. (2004). Comprehensive genomics linking between neural development and cancer: neuroblastoma as a model. *Cancer Lett* **204**: 213–224.

Pietenpol JA, Tokino T, Thiagalingam S, el-Deiry WS, Kinzler KW, Vogelstein B. (1994). Sequence-specific transcriptional activation is essential for growth suppression by p53. *Proc Natl Acad Sci USA* **91**: 1998–2002.

Roos WP, Kaina B. (2006). DNA damage-induced cell death by apoptosis. *Trends Mol Med* **12**: 440–450.

Shaw P, Freeman J, Bovey R, Iggo R. (1996). Regulation of specific DNA binding by p53: evidence for a role for *O*-glycosylation and charged residues at the carboxy-terminus. *Oncogene* **12**: 921–930.

Thomas MC, Chiang CM. (2005). E6 oncoprotein represses p53-dependent gene activation via inhibition of protein acetylation independently of inducing p53 degradation. *Mol Cell* **17**: 251–264.

Vousden KH, Lu X. (2002). Live or let die: the cell's response to p53. *Nat Rev Cancer* **2**: 594–604.

Watcharasit P, Bijur GN, Zmijewski JW, Song L, Zmijewska A, Chen X *et al.* (2002). Direct, activating interaction between glycogen synthase kinase-3beta and p53 after DNA damage. *Proc Natl Acad Sci USA* **99**: 7951–7955.

Supplementary Information accompanies the paper on the Oncogene website (http://www.nature.com/onc).

Oncogene (2008) 27, 6075-6082

www.nature.com/onc

SHORT COMMUNICATION

N-MYC promotes cell proliferation through a direct transactivation of neuronal leucine-rich repeat protein-1 (*NLRR1*) gene in neuroblastoma

MS Hossain[1,2,5], T Ozaki[1,2,5], H Wang[1,3,5], A Nakagawa[4], H Takenobu[1], M Ohira[1], T Kamijo[1] and A Nakagawara[1,2]

[1]Division of Biochemistry, Chiba Cancer Center Research Institute, Chiba, Japan; [2]Department of Molecular Biology and Oncology, Chiba University Graduate School of Medicine, Chiba, Japan; [3]Department of Pediatrics, ShengJing Hospital of China Medical University, Shenyang, People's Republic of China and [4]Department of Pathology, National Center for Child Health and Development, Tokyo, Japan

Neuronal leucine-rich repeat protein-1 (*NLRR1*) gene encodes a type I transmembrane protein with unknown function. We have previously described that *NLRR1* gene is highly expressed in unfavorable neuroblastomas as compared with favorable tumors and its higher expression levels correlate significantly with poor clinical outcome. In this study, we have found that *NLRR1* gene is one of direct target genes for N-MYC and its gene product contributes to N-MYC-dependent growth promotion in neuroblastoma. Expression levels of *NLRR1* were significantly associated with those of N-*MYC* in various neuroblastoma cell lines as well as primary neuroblastoma tissues. Indeed, enforced expression of N-MYC resulted in a remarkable induction of the endogenous *NLRR1*. Consistent with these results, we have identified two functional E-boxes within the promoter region and intron 1 of *NLRR1* gene. Intriguingly, c-myc also transactivated *NLRR1* gene. Enforced expression of NLRR1 promoted cell proliferation and rendered cells resistant to serum deprivation. In support with these observations, small-interfering RNA-mediated knockdown of the endogenous *NLRR1*-reduced growth rate and sensitized cells to serum starvation. Collectively, our present findings provide a novel insight into understanding molecular mechanisms behind aggressive neuroblastoma with N-*MYC* amplification.

Oncogene (2008) **27**, 6075–6082; doi:10.1038/onc.2008.200; published online 30 June 2008

Keywords: c-myc; neuroblastoma; N-MYC; NLRR1; proliferation; transactivation

In a sharp contrast to c-*myc*, the expression of N-*MYC* is largely restricted to embryonic tissues and neuroendocrine tumors (Boon *et al*., 2001). It has been established that N-*MYC* gene amplification is strongly associated with poor clinical outcome of aggressive human neuroblastoma (Kohl *et al*., 1983; Schwab *et al*., 1983; Seeger *et al*., 1985). Indeed, enforced expression of N-*MYC* in neuroblastoma cell lines resulted in an accelerated proliferation (Bernards *et al*., 1986; Lutz *et al*., 1996), whereas treatment of neuroblastoma cells with antisense oligonucleotides specific to N-*MYC* decreased their proliferation (Negroni *et al*., 1991). Consistent with these observations, transgenic mice overexpressing N-*MYC* in neural crest-derived tissues displayed frequent development of neuroblastomas (Weiss *et al*., 1997), suggesting that deregulated expression of N-MYC is causative in genesis and development of neuroblastoma *in vivo*. However, it is still unclear how N-MYC contributes to the formation of neoplastic phenotypes of neuroblastoma.

N-MYC is a nuclear transcription factor containing NH_2-terminal transactivation domain and COOH-terminal helix-loop-helix/leucine-zipper domain as well as the basic region (Kouzarides and Ziff, 1988; Landschulz *et al*., 1988; Murre *et al*., 1989). N-MYC forms a heterodimeric complex with Max through their helix-loop-helix/leucine-zipper domains and binds to consensus site known as E-box (CACGTG) (Alex *et al*., 1992; Blackwood *et al*., 1992; Torres *et al*., 1992). Identification of its direct transcriptional target gene(s) might provide a novel insight into understanding the functional contribution of N-MYC in malignant phenotypes of aggressive neuroblastoma. Extensive efforts demonstrated that prothymosin-α, ornithine decarboxylase teromerase reverse transcriptase, *Id2* and genes involved in ribosome biogenesis are transcriptional targets of N-MYC (Lutz *et al*., 1996; Wang *et al*., 1998; Lasorella *et al*., 2000; Boon *et al*., 2001). Recently, Slack *et al*. (2005) described that MDM2 that acts as an E3 ubiquitin protein ligase for tumor suppressor, p53, is a putative transcriptional target of N-MYC. According to their results, N-MYC directly binds to a consensus E-box within human *MDM2* promoter region and N-MYC has an ability to transactivate *MDM2* promoter. Furthermore, the endogenous MDM2 increased in N-MYC-inducible neuroblastoma cells. These observations suggest that MDM2 is important in N-MYC-driven neuroblastoma development.

Correspondence: Dr A Nakagawara, Division of Biochemistry, Chiba Cancer Center Research Institute, 666-2 Nitona, Chuoh-ku, Chiba 260-8717, Japan.
E-mail: akiranak@chiba-cc.jp
[5]These authors contributed equally to this work.
Received 28 February 2008; revised 30 April 2008; accepted 22 May 2008; published online 30 June 2008

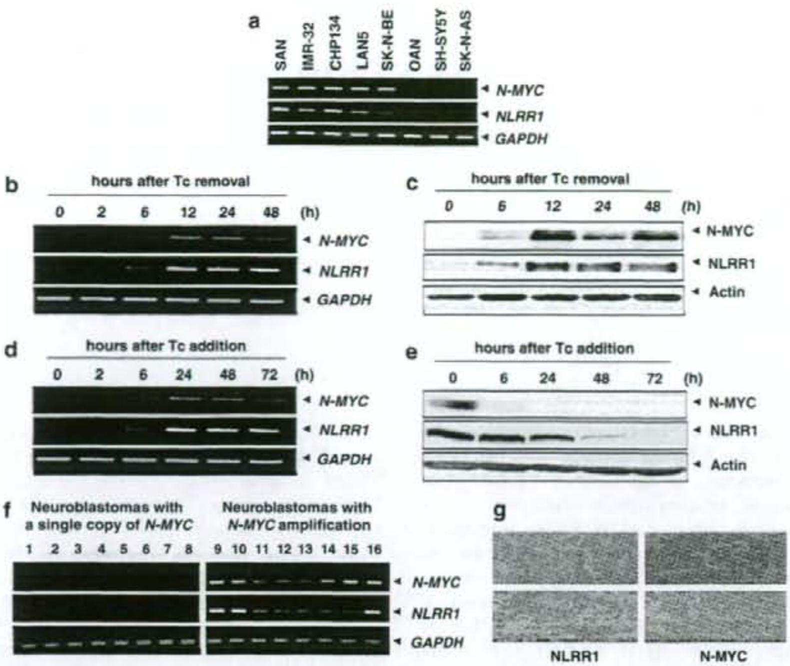

Figure 1 Expression of N-*MYC* and neuronal leucine-rich repeat protein-1 (*NLRR1*) in various neuroblastoma-derived cell lines and primary tissues. (**a**) Expression of *NLRR1* is restricted in neuroblastoma cell lines with N-*MYC* amplification. Total RNA was prepared from neuroblastoma cell lines with N-*MYC* amplification (SAN, IMR-32, CHP134, LAN5 and SK-N-BE) and neuroblastoma cell lines bearing a single copy of N-*MYC* (OAN, SH-SY5Y and SK-N-AS) using RNeasy Mini Kit (Qiagen, Valencia, CA, USA) and analysed for expression levels of N-*MYC* (top) and *NLRR1* (middle) by reverse transcription (RT)–PCR. *GAPDH* was used as an internal control (bottom) The oligonucleotide primer sequences used in this study are as follows: human *NLRR1*, 5′-GTCGATGTCCATGAATACAACCT-3′ (sense) and 5′-CAAGGCTAATGACGGCAAAC-3′ (antisense); human *N-MYC*, 5′-CTTCGGTCCAGCTTTCTCAC-3′ (sense) and 5′-GTCCGAGCGTGTTCAATTTT-3′ (antisense); human *GAPDH*, 5′-ACCTGACCTGCCGTCTAGAA-3′ (sense) and 5′-TCCACCACCCTGTTGCTGTA-3′ (antisense). (**b**, **c**) Induction of NLRR1 in N-*MYC*-inducible Tet21N cells. At the indicated time points after removal of tetracycline (Tc), total RNA and cell lysates were prepared and processed for RT–PCR (**b**) and immunoblotting with anti-N-MYC (Ab-1, Oncogene Research Products, Cambridge, MA, USA), anti-NLRR1 and anti-actin (20–33, Sigma, St Louis, MO, USA) antibodies (**c**), respectively. For RT–PCR, *GAPDH* was used as an internal control. For immunoblotting, actin was used as a loading control. (**d**, **e**) Downregulation of NLRR1 in Tet21N cells maintained in the presence of Tc. At the indicated time periods after the addition of Tc (100 ng/ml), total RNA and cell lysates were prepared and subjected to RT–PCR (**d**) and immunoblotting (**e**), respectively. (**f**) Expression of *NLRR1* in primary neuroblastomas. Total RNA was prepared from eight favorable neuroblastomas (cases 1–8) and eight unfavorable ones (cases 9–16) and subjected to RT–PCR to examine expression levels of N-*MYC* (top) and *NLRR1* (middle). *GAPDH* was used as an internal control (bottom). (**g**) Immunohistochemical analysis. Primary neuroblastomas tissues with *N-MYC* amplification were immunostained with anti-NLRR1 (left panels) or with anti-N-MYC antibody (right panels). The BenchMark XT immunostainer (Ventana Medical Systems, Tucson, AZ, USA) and 3,3′ diaminobenzidine detection kit (Ventana Medical Systems) were used to visualize NLRR1 and N-MYC. All patients agreed to participate and provided written informed consent and our present study was approved by institutional ethical review committee.

Mammalian neuronal leucine-rich repeat protein family (NLRR) is a type I transmembrane protein with extracellular leucine-rich repeats, which is composed of NLRR1-5 (Taguchi *et al*., 1996; Taniguchi *et al*., 1996; Hamano *et al*., 2004; Bando *et al*., 2005). NLRR proteins have been proposed to function as cell adhesion or signaling molecules (Fukamachi *et al*., 2002). We have previously reported that expression levels of *NLRR1* are significantly higher in unfavorable neuroblastoma than those in favorable one and higher expression levels of *NLRR1* closely correlate with poor clinical outcome of patients with neuroblastoma (Hamano *et al*., 2004). In contrast, *NLRR3* and *NLRR5* were expressed at higher levels in favorable neuroblastoma as compared with unfavorable one. For *NLRR2*, no significant differences were observed in its expression levels between favorable and unfavorable neuroblastomas (Hamano *et al*., 2004). In the present study, we have found that *NLRR1* is a direct transcriptional target of N-MYC and its gene product is important in the regulation of neuroblastoma cell proliferation.

To examine a possible correlation between expression levels of N-*MYC* and *NLRR1* in neuroblastoma cells, total RNA was prepared from the indicated cell lines and subjected to reverse transcription (RT)–PCR. As shown in Figure 1a, all neuroblastoma cell lines with N-*MYC* amplification that we examined expressed *NLRR1* mRNA, whereas we did not detect *NLRR1* mRNA in OAN, SH-SY5Y and SK-N-AS cells bearing a single copy of N-*MYC* under our experimental conditions. To confirm a possible relationship between N-*MYC* and *NLRR1*, we employed N-*MYC*-inducible neuroblastoma cells (Tet21N) derived from parental neuroblastoma cell line SHEP (Lutz *et al*., 1996). According to their results, Tet21N cells constitutively expressed N-*MYC* in the absence of tetracycline (Tc), whereas the addition of Tc to the culture decreased N-*MYC* expression levels. For this purpose, we have generated polyclonal antibody against NLRR1 that recognizes the region including amino-acid residues between positions 693 and 712. At the indicated time points after Tc depletion, total RNA and cell lysates were prepared and subjected to RT–PCR and immunoblotting, respectively. As shown in Figure 1b, Tc deprivation led to an induction of N-*MYC* in association with a significant increase in expression levels of *NLRR1*. Similar results were also obtained in immunoblotting analysis (Figure 1c). In contrast to the withdrawal of Tc, the addition of Tc to the culture significantly reduced expression levels of N-*MYC* and the concomitant decrease in expression levels of *NLRR1* was detectable at mRNA and protein levels (Figures 1d and e), suggesting that *NLRR1* might be a direct transcriptional target of N-MYC.

Consistent with these results, *NLRR1* expression was undetectable in favorable primary neuroblastomas carrying a single copy of N-*MYC*, whereas unfavorable primary neuroblastomas bearing N-*MYC* amplification expressed substantial amounts of *NLRR1* (Figure 1f). Immunohistochemical analyses also revealed that NLRR1 is coexpressed with N-MYC in primary neuroblastomas bearing N-*MYC* amplification (Figure 1g). On the other hand, NLRR1 was undetectable in primary neuroblastomas carrying a single copy of *N-MYC* (data not shown). In addition, Spearman's rank correlation coefficient between *NLRR1* and *MYCN* mRNA expression in 136 primary neuroblastomas was 0.42 ($P<0.0001$) as shown in the scatter plot of Supplementary Figure S1, suggesting that *NLRR1* and *MYCN* expression in primary tumors is also positively correlated.

To address whether N-MYC could enhance the transcription of *NLRR1*, HeLa cells were transfected with or without the increasing amounts of the expression plasmid encoding N-MYC. As clearly shown in Supplementary Figure S2, N-MYC had an ability to transactivate the endogenous *NLRR1* in a dose-dependent manner. In contrast, N-MYC had undetectable effects on expression levels of the endogenous *NLRR2* (data not shown). Intriguingly, c-myc was also capable to transactivate the endogenous *NLRR1* (Supplementary Figure S2). Expression levels of *cyclin* E were examined as a positive control. As it has been well established that N-MYC recognizes and binds to so-called E-box (5′-CACGTG-3′), we sought to find out the putative E-box sequence(s) within 5′-upstream region as well as intron 1 of *NLRR1* gene. Finally, we found out three (E-1, E-2 and E-3) and two candidate E-boxes (E-4 and E-5) within 5′-upstream region and intron 1 of *NLRR1* gene, respectively (Figure 2a). To investigate whether these canonical E-boxes could respond to N-MYC, we subcloned genomic fragments containing each of these putative E-boxes into luciferase reporter plasmid to give pluc-E1, pluc-E2, pluc-E3, pluc-E4 and pluc-E5. SK-N-AS cells carrying a single copy of N-*MYC* were co-transfected with the constant amount of the expression plasmid for N-MYC and *Renilla* luciferase reporter plasmid together with the indicated luciferase reporter plasmids. At 48 h after transfection, cells were lysed and their luciferase activities were measured. As shown in Figure 2b, E-1 and E-4 boxes showed the relatively higher luciferase activities than those of the remaining putative E-box-containing fragments. Similar results were also obtained in mouse neuroblastoma Neuro2a cells (data not shown). Thus, we focused our attention on E-1 and E-4 boxes. To verify the functional significance of E-1 and/or E4 box, we have disrupted E-1 or E-4 box to give pluc-E1Δ or pluc-E4Δ luciferase reporter construct. Luciferase reporter assays demonstrated that pluc-E1Δ and pluc-E4Δ do not respond to exogenously expressed N-MYC (Figure 2c). These results indicate that E-1 and E-4 boxes are the functional elements involved in N-MYC-dependent transcriptional activation of *NLRR1*.

To ask whether N-MYC could be recruited onto E-1 and/or E-4 box in cells, we performed chromatin immunoprecipitation (ChIP) assays. Cross-linked chromatin prepared from the indicated cells was immunoprecipitated with normal mouse serum or with monoclonal anti-N-MYC antibody. Under our experimental conditions, an average length of sonicated genomic DNA fragments was 200–800 nucleotides in length (data not shown). The genomic DNA was purified from immunoprecipitates and amplified by PCR. As shown in Figure 2d, the estimated sizes of PCR products containing E-1 or E-4 box were detectable in IMR-32, SAN and CHP134 cells with N-*MYC* amplification, whereas our ChIP assays did not detect the estimated PCR products in SK-N-AS and SH-SY5Y cells bearing a single copy of N-*MYC*. In addition, we could not detect the efficient recruitment of N-MYC onto E-3 box that did not respond to exogenously expressed N-MYC. Consistent with these results, the anti-N-MYC immunoprecipitates prepared from Tet21N cells maintained in the absence of Tc contained the genomic fragments encompassing E-1 and E-4 boxes. In a sharp contrast, genomic fragment including E-3 box was not detectable in the anti-N-MYC immunoprecipitates prepared from Tet21N cells cultured in the absence of Tc. These observations suggest that N-MYC is recruited onto E-1 and E-4 boxes of *NLRR1* gene in cells.

We next examined a possible effect of NLRR1 on cell growth of neuroblastoma cells. SK-N-BE cells were transfected with the empty plasmid or with the expression plasmid for Myc-tagged NLRR1 (NLRR1-Myc). At 48 h after transfection, cells were transferred into fresh medium containing G418 for 2 weeks.

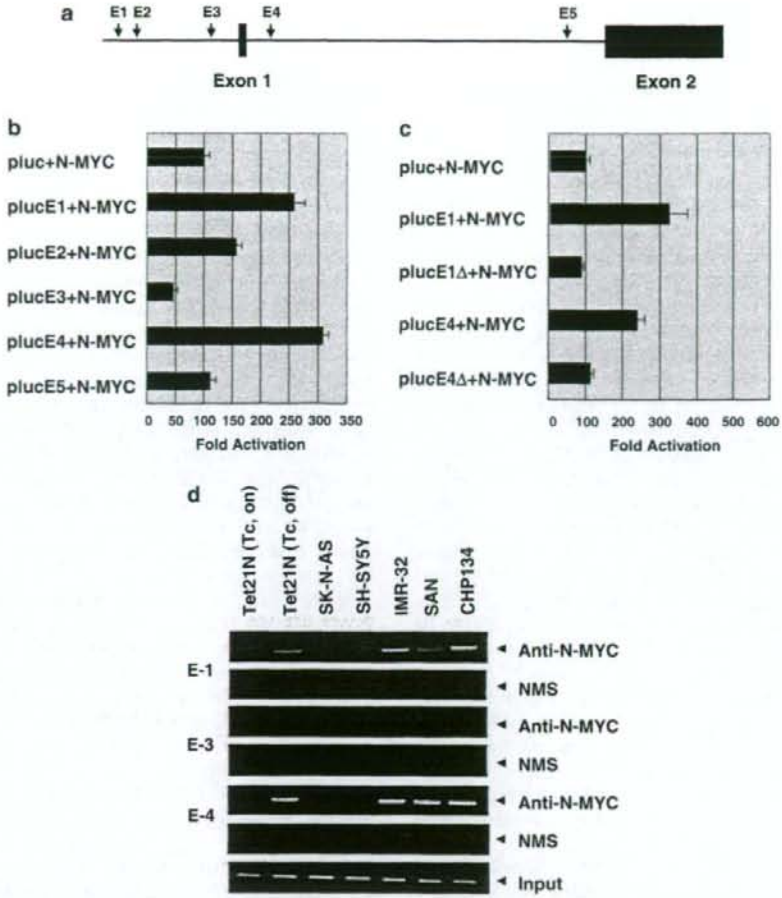

Figure 2 Luciferase reporter analysis. (**a**) Schematic drawing of the 5′-upstream region and intron 1 of human Neuronal leucine-rich repeat protein-1 (*NLRR1*) gene. Exons 1 and 2 were indicated by solid boxes. The positions of putative E-boxes were indicated by arrows. (**b**) Luciferase reporter assays. SK-N-AS cells were co-transfected with the constant amount of N-MYC-expression plasmid (100 ng), *Renilla* luciferase reporter plasmid (pRL-TK, 10 ng) and luciferase reporter plasmid containing E-1, E-2, E-3, E-4 or E-5 box (100 ng). Total amount of plasmid DNA per transfection was kept constant (510 ng) with pcDNA3. At 48 h after transfection, cells were lysed and their luciferase activities were measured by Dual-Luciferase reporter system (Promega, Madison, WI, USA). The firefly luminescence signal was normalized based on the *Renilla* luminescence signal. The results were obtained at least three independent experiments. (**c**) E-1 and E-4 boxes are required for N-MYC-dependent transactivation of *NLRR1* promoter. SK-N-AS cells were co-transfected with the constant amount of the expression plasmid for N-MYC (100 ng), pRL-TK (10 ng) and luciferase reporter plasmid lacking E-1 (pluc-E1Δ) or E-4 box (pluc-E4Δ). At 48 h after transfection, cells were lysed and their luciferase activities were measured as in (**b**). (**d**) N-MYC is efficiently recruited onto E-1 and E-4 boxes. Chromatin immunoprecipitation (ChIP) assays were carried out using chromatin immunoprecipitation assay kit provided from Upstate (Charlottesville, VA, USA). In brief, the indicated cells were cross-linked with formaldehyde and cross-linked chromatin was sonicated followed by immunoprecipitation with normal mouse serum (NMS) or with monoclonal anti-N-MYC antibody. Genomic DNAs were purified from the immunoprecipitates and subjected to PCR to amplify the genomic region containing E-1, E-3 and E-4 boxes. The oligonucleotide primer sequences used in this study are as follows: E-1, 5′-AAGTTGGATTTGATGACTGATACG-3′ (sense) and 5′-AGGCAAGAGACCATGTGCAGGAG-3′ (antisense); E-3, 5′-ATGAATCGAACAGTGGAGAGAC-3′ (sense) and 5′-AATGCTTAGGACAGTGCTTAG-3′ (antisense); E-4, 5′-TGTCTA ACATTAGCTGCGTGACC-3′ (sense) and 5′-AATGCTGTTCCGTGAATAGGTTC-3′ (antisense).

Drug-resistant cells were collected and their growth was examined. As shown in Figure 3a, exogenous NLRR1-Myc was expressed in drug-resistant cells transfected with NLRR1-Myc expression plasmid. Of note, NLRR1-Myc transfectants displayed an accelerated proliferation as compared with the control transfectants ($P<0.01$; Figure 3b). To investigate the possible role of the endogenous NLRR1, we have designed small-interfering RNA (siRNA) against NLRR1. As shown in Figure 3c, siRNA-targeting NLRR1 significantly downregulated the expression levels of the endogenous NLRR1 in SK-N-BE cells. As expected, siRNA-mediated knockdown of the endogenous NLRR1 significantly reduced the rate of cell growth as compared

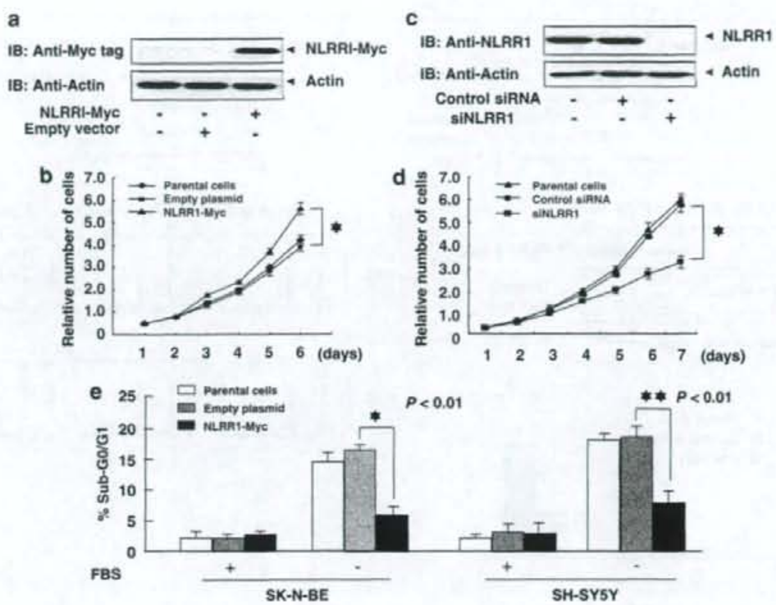

Figure 3 Neuronal leucine-rich repeat protein-1 (NLRR1) promotes cell proliferation. (**a**) Exogenous expression of NLRR1-Myc in SK-N-BE cells. SK-N-BE cells were transfected with the empty plasmid or with the expression plasmid for Myc-tagged NLRR1 (NLRR1-Myc) using Lipofectamine 2000 transfection reagent (Invitrogen, Carlsbad, CA, USA). At 48 h after transfection, cells were transferred into fresh medium containing G418 (600 μg/ml). After 2 weeks of selection, drug-resistant cells were harvested and analysed for the expression of exogenous NLRR1-Myc by immunoblotting with anti-Myc tag (PL14, Medical & Biological Laboratories, Nagoya, Japan) antibody. (**b**) Growth curves. Parental cells, control transfectants and NLRR1-Myc transfectants were seeded at a density of 1×10^5 cells per cell culture dish and allowed to attach overnight (day 1). At the indicated time points after seeding the cells, number of viable cells were measured and presented by graphs. Solid diamonds, squares and triangles indicate parental cells, control and NLRR1-Myc transfectants, respectively. *$P<0.01$. (**c**) Small-interfering RNA (siRNA)-mediated knockdown of the endogenous NLRR1. SK-N-BE cells were transfected with control siRNA or with siRNA against NLRR1 (20 nM, Takara, Ohtsu, Japan) using Lipofectamine RNAiMAX (Invitrogen). At 48 h after transfection, cell lysates were prepared and subjected to immunoblotting with anti-NLRR1 antibody. (**d**) Growth curves. SK-N-BE cells were transfected as in (**c**). At 24 h after transfection, attached cells were collected and seeded at a density of 1×10^5 cells per cell culture plates. At the indicated time points after seeding the cells, number of viable cells were measured and presented by graphs. Solid triangles, circles and squares indicate parental cells, control transfectants and NLRR1-knocked down cells, respectively. *$P<0.01$. (**e**) NLRR1 has an anti-apoptotic potential in response to fetal bovine serum (FBS) starvation. SK-N-BE and SH-SY5Y cells were transfected with the empty plasmid or with the expression plasmid encoding NLRR1-Myc. At 48 h after transfection, cells were transferred into fresh medium containing G418 (600 μg/ml). After 2 weeks of selection, drug-resistant cells were harvested and cultured in the presence or absence of FBS. At 24 h after treatment, floating and attached cells were collected, stained with propidium iodide (PI) and their cell-cycle distributions were analysed by fluorescence-activated cell sorting (FACS, Becton Dickinson, Mountain View, CA, USA). Results obtained by FACS analysis were presented by graphs. Open, gray and solid boxes indicate parental cells, control transfectants and NLRR1-Myc-expressing transfectants, respectively. *$P<0.01$, **$P<0.01$.

with the control cells ($P<0.01$; Figure 3d), indicating that NLRR1 has an ability to promote cell growth in neuroblastoma.

As described previously (Hamano *et al.*, 2004), *NLRR1* was expressed at significantly higher levels in unfavorable neuroblastoma than favorable one, indicating that NLRR1 might have an anti-apoptotic activity. To address this issue, SK-N-BE and SH-SY5Y cells were transfected with the empty plasmid or with the expression plasmid for NLRR1-Myc. At 48 h after transfection, cells were exposed to G418 for 2 weeks. Drug-resistant cells were collected and cultured in the presence or absence of fetal bovine serum (FBS). At 24 h after FBS starvation, floating and attached cells were harvested, stained with propidium iodide and measured number of cells with sub-G_0/G_1 DNA content by fluorescence-activated cell sorting (FACS) analysis. As shown in Figure 3e, FBS deprivation increased number of parental and control SK-N-BE cells with sub-G_0/G_1 DNA content as compared with those cultured in the presence of FBS, whereas enforced expression of NLRR1-Myc significantly decreased number of cells with sub-G_0/G_1 DNA content relative to parental and control cells under FBS deprivation. Similar results were also obtained in SH-SY5Y cells (Figure 3e).

In support with these results, cleaved caspase-3 was detectable in control SK-N-AS transfectants maintained in the absence of FBS, whereas we did not detect cleaved caspase-3 in NLRR1-Myc transfectants under FBS deprivation (Figure 4a). Cleaved caspase-3 was also detected in parental cells in the absence of FBS (Figure 4b). In addition, cleaved poly-(ADP-ribose)

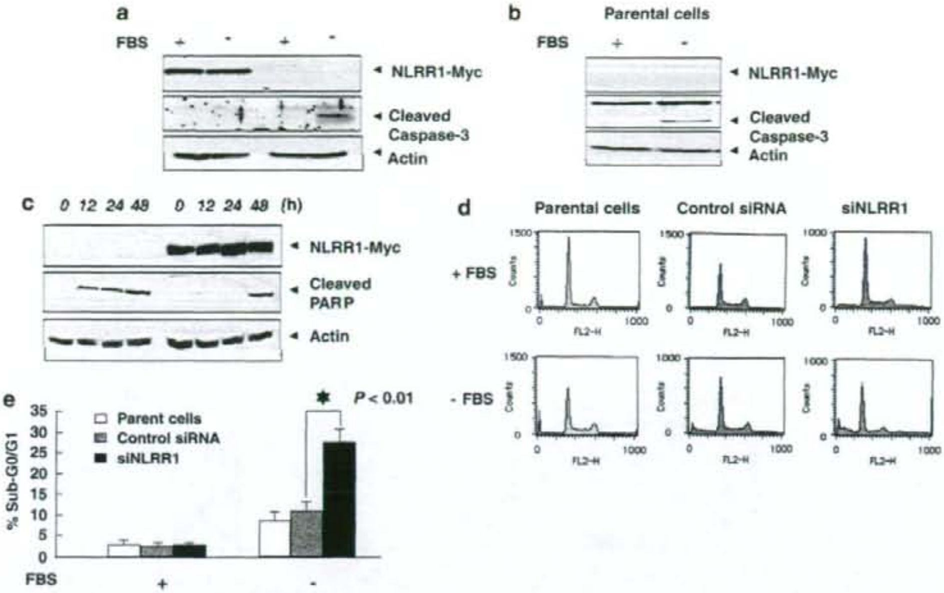

Figure 4 Neuronal leucine-rich repeat protein-1 (NLRR1) is involved in the regulation of serum starvation-induced apoptosis. (**a**) NLRR1 inhibits the activation of caspase-3. Control transfectants and NLRR1-Myc-expressing transfectants derived from SK-N-AS cells were cultured in the presence or absence of fetal bovine serum (FBS). At 24 h after the treatment, cell lysates were prepared and processed for immunoblotting with anti-Myc tag (top) or with anti-caspase-3 (Cell Signaling, Beverly, MA, USA) antibody (middle). Actin was used as a loading control (bottom). (**b**) Deprivation of FBS induces cleavage of caspase-3 in SK-N-AS cells. SK-N-AS cells were cultured in the presence or in the absence of FBS. At 24 h after the treatment, cell lysates were prepared and subjected to immunoblotting with the indicated antibodies. (**c**) Effect of NLRR1 on cleavage of poly-(ADP-ribose) polymerase (PARP) in response to FBS deprivation. Control transfectants (left) and NLRR1-Myc-expressing transfectants (right) were maintained in the absence of FBS. At the indicated time points after FBS withdrawal, cell lysates were prepared and analysed for the expression of NLRR1-Myc (top) as well as the proteolytic cleavage of PARP by immunoblotting with anti-PARP (Cell Signaling) antibody (middle). Actin was used as a loading control (bottom). (**d**, **e**) Small-interfering RNA (siRNA)-mediated knockdown of the endogenous NLRR1 enhances apoptosis in response to FBS starvation. Tet21N cells were grown in the fresh medium without tetracycline (Tc) and transfected with control siRNA or with siRNA against NLRR1. At 48 h after transfection, cells were transferred into fresh medium without Tc and FBS. At 24 h after FBS starvation, floating and attached cells were collected, stained with propidium iodide (PI) and their cell-cycle distributions were examined by fluorescence-activated cell sorting (FACS) (**d**). Results obtained by FACS analysis were presented by graphs. Open, gray and solid boxes indicate parental cells, control transfectants and NLRR1-knocked down transfectants, respectively (**e**). $^{*}P<0.01$.

polymerase (PARP) that is one of caspase-3 substrates (Truscott *et al*., 2007), started to be observed in control transfectants 12 h after FBS starvation (Figure 4c). On the other hand, the kinetics for cleavage of PARP was delayed in NLRR1-Myc transfectants. Under our experimental conditions, control SK-N-AS transfectants underwent apoptosis in response to FBS deprivation, whereas enforced expression of NLRR1-Myc in SK-N-AS cells inhibited the FBS deprivation-induced apoptosis (data not shown). These findings suggest that NLRR1 confers resistance of neuroblastoma cells to FBS starvation-induced apoptosis.

To further confirm this notion, Tet21N cells were maintained in the absence of Tc and then transfected with control siRNA or with siRNA against NLRR1. At 48 h after transfection, cells were cultured in the absence of FBS for 24 h and then their cell-cycle distributions were analysed by FACS. As shown in Figures 4d and e, siRNA-mediated knockdown of the endogenous NLRR1 resulted in a significant increase in number of cells with sub-G_0/G_1 DNA content in response to FBS deprivation as compared with parental cells and control transfectants. Collectively, our present results strongly suggest that NLRR1 is a novel transcriptional target of N-MYC and has a growth-promoting as well as anti-apoptotic potential.

Small-interfering RNA-mediated knockdown of the endogenous NLRR1 in SK-N-BE cells bearing N-*MYC* amplification resulted in a significant decrease in the rate of cell growth. Furthermore, enforced expression of NLRR1-Myc conferred resistance of SK-N-BE and SH-SY5Y cells to FBS deprivation-mediated apoptosis. In contrast, siRNA-mediated knockdown of the endogenous NLRR1 led to an increase in number of cells with sub-G_0/G_1 DNA content in response to FBS deprivation. In addition, NLRR1-Myc blocked the activation of caspase-3 in SK-N-AS cells exposed to FBS depletion and thereby inhibiting the proteolytic cleavage of PARP. Thus, it is conceivable that NLRR1 inhibits the mitochondria-dependent intrinsic apoptotic pathway of caspase activation (Degterev *et al*., 2003). As reported previously (Hamano *et al*., 2004), expression levels of *NLRR1* in unfavorable neuroblastoma were significantly higher than those of favorable one and closely correlated with poor clinical outcome. As aggressive neuroblastoma displays unfavorable clinical outcome despite intensive chemotherapy (Brodeur and Nakagawara, 1992), it is likely that N-MYC-mediated induction of NLRR1 is involved in the regulation of chemoresistant phenotypes of certain neuroblastomas. However, precise molecular mechanisms behind NLRR1-mediated growth promotion and anti-apoptotic effect in response to FBS starvation remain unclear. Further studies should be necessary to address this issue.

According to our present results, N-MYC-dependent transcriptional induction of *NLRR1* was observed in neuroblastoma cell lines. Furthermore, expression levels of *NLRR1* significantly correlated with those of N-*MYC* in primary neuroblastomas. Intriguingly, the enforced expression of N-MYC in HeLa cells also induced the expression of NLRR1, indicating that N-MYC-mediated transcriptional activation of *NLRR1* is not restricted to neuroblastoma cells. As described previously (Blackwood and Eisenman, 1991; Torres *et al*., 1992), c-myc/Max heterodimeric complex also recognizes and binds to E-box. Like N-MYC, c-myc had an ability to induce the expression of NLRR1. Of note, our luciferase reporter assays indicated that E-1 and E-4 boxes are required for N-MYC-dependent activation of *NLRR1* promoter, whereas E-3 box does not respond to N-MYC. Similar results were also obtained in cells transfected with the expression plasmid for c-myc (data not shown). As described previously (Hamano *et al*., 2004), *NLRR1* was expressed ubiquitously in human tissues. Among them, higher levels of *NLRR1* expression were observed in nerve tissues. Considering that N-*MYC* expression is largely restricted to embryonic tissues as well as neuroendocrine tumors, whereas c-*myc* is expressed in a wide variety of tissues as well as tumors (Boon *et al*., 2001), N-MYC and c-myc might act as transcription factors for *NLRR1* in a cell-type-dependent manner under physiological conditions.

In the present study, we have found that *NLRR1* is one of direct transcriptional targets of oncogenic N-MYC and is important in the regulation of cell proliferation and the protection of cells from FBS deprivation-induced apoptosis in neuroblastoma cells. In support with this notion, there exists a positive correlation between expression levels of N-*MYC* and *NLRR1* in primary neuroblastomas. To our knowledge, NLRR1 is a first membrane protein whose expression levels are directly regulated by N-MYC. Thus, our present findings might provide a novel insight into understanding molecular mechanisms behind genesis and development of aggressive neuroblastoma with N-*MYC* amplification.

Acknowledgements

We are grateful to Dr M Schwab for providing the expression plasmid for N-MYC. We thank Ms Y Nakamura for technical assistance. This work was supported in part by a Grant-in-Aid from the Ministry of Health, Labour and Welfare for Third Term Comprehensive Control Research for Cancer, a Grant-in-Aid for Scientific Research on Priority Areas from the Ministry of Education, Culture, Sports, Science and Technology, Japan, a Grant-in-Aid for Scientific Research from Japan Society for the Promotion of Science, Uehara Memorial Foundation and Hisamitsu Pharmaceutical Co.

References

Alex R, Sozeri O, Meyer S, Dildrop R. (1992). Determination of the DNA sequence recognized by the bHLH-zip domain of the N-Myc protein. *Nucleic Acids Res* **20**: 2257–2263.

Bando T, Sekine K, Kobayashi S, Watabe AM, Rump A, Tanaka M *et al*. (2005). Neuronal leucine-rich repeat protein 4 functions in hippocampus-dependent long-lasting memory. *Mol Cell Biol* **25**: 4166–4175.

Bernards R, Dessain SK, Weinberg RA. (1986). N-myc amplification causes down-modulation of MHC class I antigen expression in neuroblastoma. *Cell* **47**: 667–674.

Blackwood EM, Eisenman RN. (1991). Max: a helix-loop-helix zipper protein that forms a sequence-specific DNA binding complex with Myc. *Science* **251**: 1211–1217.

Blackwood EM, Kretzner I, Eisenman RN. (1992). Myc and Max function as a nucleoprotein complex. *Curr Opin Genet Dev* **2**: 227–235.

Boon K, Caron HN, van Asperen R, Valentijn L, Hermus MC, van Sluis P *et al*. (2001). N-myc enhances the expression of a large set of genes functioning ribosome biogenesis and protein synthesis. *EMBO J* **20**: 1383–1393.

Brodeur GM, Nakagawara A. (1992). Molecular basis of clinical heterogeneity in neuroblastoma. *Am J Pediatr Hematol Oncol* **14**: 111–116.

Degterev A, Boyce M, Yuan J. (2003). A decade of caspases. *Oncogene* **22**: 8543–8567.

Fukamachi K, Matsuoka Y, Ohno H, Hamaguchi T, Tsuda H. (2002). Neuronal leucine-rich repeat protein-3 amplifies MAPK activation by epidermal growth factor through a carboxyl-terminal region containing endocytosis motifs. *J Biol Chem* **277**: 43549–43552.

Hamano S, Ohira M, Isogai E, Nakada K, Nakagawara A. (2004). Identification of novel human neuronal leucine-rich repeat (h*NLRR*) family, genes and inverse association of expression of *Nbla10449*/h*NLRR-1* and *Nbla10677*/h*NLRR-3* with the prognosis of primary neuroblastomas. *Int J Oncol* **24**: 1457–1466.

Kohl NE, Kanda N, Schreck RR, Bruns G, Latt SA, Gilbert F *et al*. (1983). Transposition and amplification of oncogene-related sequences in human neuroblastomas. *Cell* **35**: 359–367.

Kouzarides T, Ziff E. (1988). The role of the leucine zipper in the fos-jun interaction. *Nature* **336**: 646–651.

Landschulz WH, Johnson PF, McKnight S. (1988). The leucine zipper: a hypothetical structure common to a new class of DNA binding proteins. *Science* **240**: 1759–1764.

Lasorella A, Noseda M, Beyna M, Iavarone A. (2000). Id2 is a retinoblastoma protein target and mediates signaling by Myc oncoproteins. *Nature* **407**: 592–598.

Lutz W, Stohr M, Schurmann J, Wenzel A, Lohr A, Schwab M. (1996). Conditional expression of N-myc in human neuroblastoma cells increases expression of a-prothymosin and ornithine decarboxylase and accelerates progression into S-phase early after mitogenic stimulation of quiescent cells. *Oncogene* **13**: 803–812.

Murre C, Schonleber McCaw P, Baltimore D. (1989). A new DNA binding and dimerization motif in immunoglobulin enhancer binding, daughterless, MyoD, and myc proteins. *Cell* **56**: 777–783.

Negroni A, Scarpa S, Romeo A, Ferrari S, Modesti A, Raschella G. (1991). Decrease of proliferation rate and induction of differentiation by a MYCN antisense DNA oligomer in a human neuroblastoma cell line. *Cell Growth Differ* **2**: 511–518.

Schwab M, Alitalo K, Klempnauer KH, Varmus HE, Bishop JM, Gilbert F *et al.* (1983). Amplified DNA with limited homology to *myc* cellular oncogene is shared by human neuroblastoma cell lines and a neuroblastoma tumour. *Nature* **305**: 245–248.

Seeger RC, Brodeur GM, Sather H, Dalton A, Siegel SE, Wong KY *et al.* (1985). Association of multiple copies of the N-myc oncogene with rapid progression of neuroblastomas. *N Engl J Med* **313**: 1111–1116.

Slack A, Chen Z, Tonelli R, Pule M, Hunt L, Pession A *et al.* (2005). The p53 regulatory gene MDM2 is a direct transcriptional target of MYCN in neuroblastoma. *Proc Natl Acad Sci USA* **102**: 731–736.

Taguchi A, Wanaka A, Mori T, Matsumoto K, Imai Y, Takagi T *et al.* (1996). Molecular cloning of novel leucine-rich repeat proteins and their expression in the developing mouse nervous system. *Brain Res Mol Brain Res* **35**: 31–40.

Taniguchi H, Tohyama A, Takagi T. (1996). Cloning and expression of a novel gene for a protein with leucine-rich repeats in the developing mouse nervous system. *Brain Res Mol Brain Res* **36**: 45–52.

Torres R, Schreiber-Agus N, Morgenbesser SD, DePinho RA. (1992). Myc and Max: a putative transcriptional complex in search of a cellular target. *Curr Opin Cell Biol* **4**: 468–474.

Truscott M, Denault JB, Goulet B, Leduy L, Salvesen GS, Nepveu A. (2007). Carboxy-terminal proteolytic processing of CUX1 by a caspase enables transcriptional activation in proliferating cells. *J Biol Chem* **282**: 30216–30226.

Wang J, Xie I, Allan S, Beach D, Hannon G. (1998). Myc activates telomerase. *Genes Dev* **12**: 1769–1774.

Weiss WA, Aldape K, Mohapatra G, Feuerstein BG, Bishop JM. (1997). Targeted expression of MYCN causes neuroblastoma in transgenic mice. *EMBO J* **16**: 2985–2995.

Supplementary Information accompanies the paper on the Oncogene website (http://www.nature.com/onc)

Int. J. Cancer: **123**, 2087–2094 (2008)

Expression of *TSLC1*, a candidate tumor suppressor gene mapped to chromosome 11q23, is downregulated in unfavorable neuroblastoma without promoter hypermethylation

Kiyohiro Ando[1], Miki Ohira[1], Toshinori Ozaki[1], Atsuko Nakagawa[2], Kohei Akazawa[3], Yusuke Suenaga[1], Yohko Nakamura[1], Tadayuki Koda[4], Takehiko Kamijo[1], Yoshinori Murakami[5] and Akira Nakagawara[1]*

[1]*Division of Biochemistry, Chiba Cancer Center Research Institute, Chiba, Japan*
[2]*Division of Clinical Laboratory, National Center for Child Health and Development, Tokyo, Japan*
[3]*Division of Medical Information, Niigata University Medical and Dental Hospital, Niigata, Japan*
[4]*Center for Functional Genomics, Hisamitsu Pharmaceutical Co. Inc., Chiba, Japan*
[5]*Division of Molecular Pathology, Department of Cancer Biology, Institute of Medical Science, The University of Tokyo, Tokyo, Japan*

Although it has been well documented that loss of human chromosome 11q is frequently observed in primary neuroblastomas, the smallest region of overlap (SRO) has not yet been precisely identified. Previously, we performed array-comparative genomic hybridization (array-CGH) analysis for 236 primary neuroblastomas to search for genomic aberrations with high-resolution. In our study, we have identified the SRO of deletion (10-Mb or less) at 11q23. Within this region, there exists a *TSLC1/IGSF4/CADM1* gene (*Tumor suppressor in lung cancer 1/Immunoglobulin superfamily 4/Cell adhesion molecule 1*), which has been identified as a putative tumor suppressor gene for lung and some other cancers. Consistent with previous observations, we have found that 35% of primary neuroblastomas harbor loss of heterozygosity (LOH) on *TSLC1* locus. In contrast to other cancers, we could not detect the hypermethylation in its promoter region in primary neuroblastomas as well as neuroblastoma-derived cell lines. The clinicopathological analysis demonstrated that *TSLC1* expression levels significantly correlate with stage, Shimada's pathological classification, *MYCN* amplification status, *TrkA* expression levels and DNA index in primary neuroblastomas. The immunohistochemical analysis showed that TSLC1 is remarkably reduced in unfavorable neuroblastomas. Furthermore, decreased expression levels of *TSLC1* were significantly associated with a poor prognosis in 108 patients with neuroblastoma. Additionally, TSLC1 reduced cell proliferation in human neuroblastoma SH-SY5Y cells. Collectively, our present findings suggest that *TSLC1* acts as a candidate tumor suppressor gene for neuroblastoma.

Key words: *TSLC1/IGSF4/CADM1*; neuroblastoma; 11q23; tumor suppressor

Neuroblastoma is one of the most common solid tumors in childhood and originates from the sympathoadrenal lineage of neural crest. Its biological as well as clinical behavior is highly heterogeneous in different prognostic subsets. Tumors found in patients under 1 year of age often regress spontaneously or differentiate and result in a favorable prognosis.[1] In a sharp contrast to these favorable neuroblastomas, tumors found in patients over 1 year of age are often aggressive with an unfavorable prognosis despite an intensive therapy. A large number of multiple genomic aberrations including DNA index, *MYCN* amplification status, allelic loss of the distal part of chromosome 1p and the gain of chromosome 17q have been identified in neuroblastoma.[2,3]

Alternatively, allelic loss of 11q has been frequently observed in advanced stage of neuroblastoma with single copy of *MYCN*. Indeed, 30% of tumors harbor allelic loss of 11q, and it might be an independent prognostic indicator for clinically high-risk patients without *MYCN* amplification.[4,5] Aberrant deletions of 11q often occur in a distal part of its long arm. Although several lines of evidence delineated the smallest region of overlaps (SRO) of deletions at 11q, it remains unclear whether there could exist a candidate tumor suppressor gene(s) implicated in biological and clinical behaviors of neuroblastoma.[6,7] Recently, we have performed an array-comparative genomic hybridization (array-CGH) analysis using 236 primary neuroblastomas and finally defined the SRO (10-Mb or less) at 11q23.[3,8] During our extensive search for the already identified candidate tumor suppressor gene(s) within this region, we have found that *TSLC1/IGSF4/CADM1* gene is localized within this region.

TSLC1 gene has been originally identified as a putative tumor suppressor for non-small-cell lung cancer (NSCLC) located at chromosome 11q23 by functional complementation strategy of a human lung cancer cell line. The downregulation of *TSLC1* gene was frequently detected in various human cancers including NSCLC, prostate cancers, hepatocellular carcinomas and pancreatic cancers through its allelic loss as well as hypermethylation of its promoter region. In spite of an extensive mutation search, only 2 inactivating *TSLC1* gene mutations were detected in 161 primary tumors and tumor-derived cell lines, suggesting that *TSLC1* is rarely mutated in human cancers.[9] *TSLC1* encodes a single membrane-spanning glycoprotein involved in cell–cell adhesion through homophilic trans interaction.[10] Accumulating evidence indicates that TSLC1 is significantly associated with biological aggressiveness and metastasis of certain types of cancer,[11–16] whereas the functional significance of TSLC1 in neuroblastoma remains elusive.

In the present study, we have further delineated the SRO of 11q deletion in primary neuroblastoma by array-CGH analysis and finally identified *TSLC1* gene within this region. In contrast to the other cancers, hypermethylation of *TSLC1* promoter region was undetectable in neuroblastoma. Intriguingly, the expression levels of *TSLC1* gene were highly associated with clinical stage, Shimada's pathological classification, *MYCN* amplification status, *TrkA* expression levels and DNA index in primary neuroblastoma.

Additional Supporting Information may be found in the online version of this article.

Abbreviations: array-CGH, array-comparative genomic hybridization; BAC, bacterial artificial chromosome; LOH, loss of heterozygosity; PARP, poly(ADP-ribose) polymerase; SRO, smallest region of overlap; STS, sequence-tagged-site; TSA, trichostatin A; TSLC1, tumor suppressor in lung cancer 1.

Grant sponsors: Ministry of Health, Labour and Welfare for Third Term Comprehensive Control Research for Cancer; Ministry of Education, Culture, Sports, Science and Technology, Japan; Scientific Research from Japan Society for the Promotion of Science.

*Correspondence to: Chiba Cancer Center Research Institute, 666-2 Nitona, Chuo-ku, Chiba 260-8717. Fax: +81-43-265-4459.
E-mail: akiranak@chiba-cc.jp

Received 21 February 2008; Accepted after revision 19 May 2008
DOI 10.1002/ijc.23776
Published online 22 August 2008 in Wiley InterScience (www.interscience.wiley.com).

UICC global cancer control
Publication of the International Union Against Cancer

Material and methods

Patients, tumor specimens and cell lines

One hundred and eight tumor specimens used in the present study were kindly provided from various institutions and hospitals in Japan (see Supplementary Information). Informed consent was obtained at each institution or hospital. All tumors were diagnosed clinically as well as pathologically as neuroblastoma and staged according to the International Neuroblastoma Staging System (INSS) criteria.[17] Twenty-seven patients were Stage 1, 15 Stage 2, 36 Stage 3, 23 Stage 4 and 7 Stage 4S. The patients were treated by the standard protocols as described previously.[18,19] *MYCN* copy number, *TrkA* mRNA expression levels and DNA index were measured as reported previously.[20] Our present study was approved by the Institutional Review Board of the Chiba Cancer Center (CCC7817).

Human tumor-derived cell lines were cultured in RPMI 1640 medium (Nissui, Tokyo, Japan) supplemented with 10% heat-inactivated fetal bovine serum (FBS, Invitrogen, Carlsbad, CA) and 50 μg/ml penicillin/streptomycin (Invitrogen) in an incubator with humidified air at 37°C with 5% CO_2.

Array-comparative genomic hybridization

Array-CGH analysis was performed using UCSF BAC array (2464 BACs, ≈1 Mb resolution) with 236 primary neuroblastomas. Detailed experimental procedures and the criteria for losses and gains were described previously.[3,20–22]

LOH analysis

Genomic DNA prepared from neuroblastomas and bloods was amplified by PCR-based strategy using the primer set, one of which was labeled with fluorescent dye CY5. The amplified fragments including 3 polymorphic STS markers encompassing *TSLC1*, *D11S4111*, *D11S2077* and *D11S1885*, were separated by 6% polyacrylamide gels containing 6 M urea using an automated ALF express DNA sequencer.

Semiquantitative and quantitative reverse transcription-PCR analysis

Total RNA was prepared from the indicated primary neuroblastomas, various human normal tissues and tumor-derived cell lines were subjected to semiquantitative RT-PCR using SuperScript II reverse transcriptase and random primers (Invitrogen), according to the manufacturer's instructions. Oligonucleotide primer set used to amplify *TSLC1* by semiquantitative RT-PCR was as follows: 5′-CATTTTGGAATTTGCCTGCT-3′ (sense) and 5′-GGCAGCAG-CAAAGAG TTTTC-3′ (antisense). Quantitative real-time PCR was carried out using TaqMan(R) Gene Expression Assay System (Applied Biosystems, Foster City, CA) as described previously.[20] In brief, expression levels were calculated as a ratio of mRNA level for a given gene relative to mRNA for *GAPDH* in the same cDNA. The oligonucleotide primers and TaqMan probes, labeled at the 5′-end with the reporter dye 6-carboxyfluorescein (FAM) and at the 3′-end with 6-carboxytetramethylrhodamine (TAMRA), were provided by Applied Biosystems (Hs00942508_m1).

Immunohistochemistry

A 4-μm-thick section of formalin-fixed, paraffin-embedded tissues were stained with hematoxylin and eosin and the adjacent sections were immunostained for TSLC1 using polyclonal anti-TSLC1 antibody (CC2) as described previously.[10] The BenchMark XT immunostainer (Ventana Medical Systems, Tucson, AZ) and 3-3′ diaminobenzidine detection kit (Ventana Medical Systems) were used to visualize TSLC1. Appropriate positive and negative control experiments were also performed in parallel for each immunostaining.

Small interfering RNA

TSLC1 siRNA (GUCAAUAAGAGUGACGACUUU) and Stealth RNAi Negative Control Duplex were purchased from Sigma-Aldrich (St. Louis, MO) and Invitrogen, respectively.

Transfection

Neuroblastoma-derived SH-SY5Y cells were transfected with the indicated combinations of expression plasmids or with siRNA against TSLC1 using LipofectAMINE 2000 or LipofectAMINE RNAiMAX transfection reagent (Invitrogen), according to the manufacturer's recommendations.

Colony formation assay

SH-SY5Y and SK-N-AS cells (1×10^5 cells/plate) were seeded in 6-well cell culture plates and transfected with or without the increasing amounts of the expression plasmid for TSLC1 (0, 250, 750 or 1,000 ng). Total amounts of plasmid DNA per transfection were kept constant (1 μg) with the empty plasmid (pcDNA3.1-Hygro (+); Invitrogen). Forty-eight hours after transfection, cells were transferred into the fresh medium containing hygromycin (at a final concentration of 200 μg/ml) and maintained for 14 days. Drug-resistant colonies were then stained with Giemsa's solution and numbers of drug-resistant colonies were scored.

Cell growth assay

SH-SY5Y cells (6×10^5 cells/dish) were seeded in 10-cm diameter cell culture dish and transiently transfected with siRNA against TSLC1 (240 pmol). Thirty-six hours after transfection, 2×10^4 cells were transferred into 6-well plates and transfected with 60 pmol of siRNA against TSLC1. At the indicated time points after transfection, number of viable cells was measured using a Coulter Counter (Coulter Electronics, Hialeah, Finland).

Bisulfite-sequencing

Sodium bisulfite-mediated modification of genomic DNA was performed using BisulFast Methylated DNA Detection Kit (Toyobo, Osaka, Japan), according to the manufacture's instructions. Modified genomic DNA was subjected to PCR-based amplification with a primer set as described previously.[23] The PCR products containing the promoter region of *TSLC1* gene were purified by PCR Purification Kit (Qiagen, Valencia, CA) and their nucleotide sequences were determined by using a 3730 DNA Analyzer (Applied Biosystem).

Statistical analysis

Fisher's exact tests were employed to examine possible associations between *TSLC1* expression and other prognostic indicators such as age. The difference between high and low expression levels of *TSLC1* was based on the mean value obtained from quantitative real-time PCR analysis. Kaplan-Meier survival curves were calculated, and survival distributions were compared using the log-rank test. Cox regression models were used to investigate the associations between *TSLC1* expression levels, age, *MYCN* amplification status, INSS and survival. Differences were considered significant if the p-value was less than 0.05.

Results

Array-comparative genomic hybridization analysis identifies the smallest region of overlaps of deletion in neuroblastoma at 11q23

We have previously performed array-CGH analysis using UCSF BAC array (2464 BACs, ≈1-Mb resolution) and 236 primary neuroblastomas.[3] In our array-CGH study, 66 tumors were revealed to have partial deletion of 11q as shown in Figure 1*a*, whose SRO were approximately 10-Mb long at 11q23 (from physical location of 110,979 to 119,806 kb in UCSC database, May 2006). To date, the data base analysis demonstrated that there could exist approximately 100 genes within this region. Of inter-

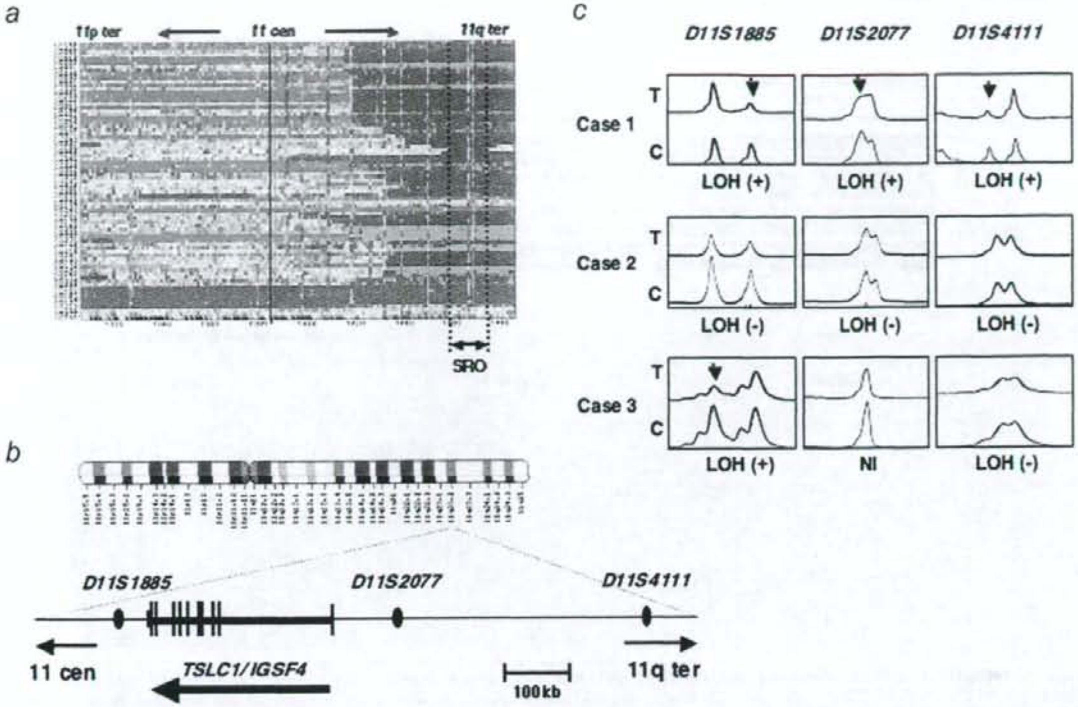

FIGURE 1 – Identification of the SRO of deletion at 11q in primary neuroblastoma. (*a*) Array-CGH analysis. Blue color indicates the position of the deleted area in each case. The smallest region of overlaps (SRO) of deletion at 11q is also shown. (*b*) The schematic drawing of the relative positions of 3 independent polymorphic markers at 11q23 used in the present study and *TSLC1* gene on human chromosome 11. (*c*) Representative electropherograms obtained from LOH analysis. Genomic DNA prepared from primary tumors (T) and their corresponding blood (C) was subjected to LOH analysis. Allelic losses are indicated by arrowheads. NI, not informative.

est, *TSLC1* gene which has been considered as a putative tumor suppressor for human lung as well as other cancers[9] locates within this region (Fig. 1*b*). These observations prompted us to perform loss of heterozygosity (LOH) as well as expression studies of *TSLC1* gene in primary neuroblastoma.

LOH at the TSLC1 locus is frequently detected in primary neuroblastoma

According to the previous observations,[9,24] tumor-specific downregulation of *TSLC1* gene might be largely attributed to loss of one allele in association with the hypermethylation of its promoter region in the remaining allele. To address whether LOH of *TSLC1* locus could be frequently detectable in primary neuroblastoma, we carried out LOH analysis using 3 independent fluorescently labeled polymorphic microsatellite markers (*D11S1885*, *D11S2077* and *D11S4111*) surrounding *TSLC1* gene (Fig. 1*b*). In accordance with the previous results,[9,25,26] the incidence of 11q23 LOH was 22% (7 of 32) and 45% (18 of 40) in favorable neuroblastomas (Stage 1 or 2) and unfavorable ones (Stage 3 or 4), respectively (data not shown). Statistical Fisher's exact test analysis revealed that the presence of LOH at this locus is associated with unfavorable neuroblastomas ($p = 0.0493$; data not shown). It is worth noting that LOH is detectable at *D11S1885* but not at *D11S4111* in Case 3 tumor (Fig. 1*c*), indicating that a putative chromosome breakpoint might exist between these loci.

Downregulation of TSLC1 expression is frequently observed in unfavorable neuroblastomas

Based on the previous observations,[11–16] the expression levels of *TSLC1* were significantly reduced in advanced stages of tumors as compared with those in early stages of tumors. We then examined the expression levels of *TSLC1* in 16 favorable neuroblastomas without *MYCN* amplification and 16 unfavorable ones with *MYCN* amplification. As clearly shown in Figure 2*a*, *TSLC1* was expressed at lower levels in unfavorable neuroblastomas relative to favorable ones as examined by semiquantitative RT-PCR. To ask whether there could exist a possible relationship between downregulation of *TSLC1* and *MYCN* amplification, we examined the expression levels of *TSLC1* in various neuroblastoma-derived cell lines bearing single copy of *MYCN* or *MYCN* amplification. As shown in Supplementary Figure 1*a*, a significant downregulation of *TSLC1* expression was detected in 2 of 6 neuroblastoma cell lines carrying single copy of *MYCN* (OAN and CNB-RT) and in 4 of 21 (CHP134, KP-N-NS, SK-N-DZ and NMB) bearing *MYCN* amplification as examined by semiquantitative RT-PCR. In addition, there was no obvious correlation between the expression levels of *TSLC1* and loss of 11q except OAN, SK-N-DZ and NMB. Next, we checked the expression levels of *TSLC1* in various human adult and fetal tissues. As seen in Supplementary Figure 1*b*, *TSLC1* was highly expressed in normal neuronal tissues, adrenal gland, testis, prostate and liver. Our present results suggest that *TSLC1* is expressed in normal neuronal tissues and its expression levels might be regulated in a *MYCN*-dependent manner in